JPRS L/8247

29 January 1979

[redacted]

USSR

[redacted]

[redacted]

TRANSLATIONS ON USSR SCIENCE AND TECHNOLOGY
PHYSICAL SCIENCES AND TECHNOLOGY
(FOUO 6/79)

U. S. JOINT PUBLICATIONS RESEARCH SERVICE

[redacted]

APPROVED FOR RELEASE: 2007/02/08: CIA-RDP82-00850R000100010054-0

NOTE

JPRS publications contain information primarily from foreign newspapers, periodicals and books, but also from news agency transmissions and broadcasts. Materials from foreign-language sources are translated; those from English-language sources are transcribed or reprinted, with the original phrasing and other characteristics retained.

Headlines, editorial reports, and material enclosed in brackets [] are supplied by JPRS. Processing indicators such as [Text] or [Excerpt] in the first line of each item, or following the last line of a brief, indicate how the original information was processed. Where no processing indicator is given, the information was summarized or extracted.

Unfamiliar names rendered phonetically or transliterated are enclosed in parentheses. Words or names preceded by a question mark and enclosed in parentheses were not clear in the original but have been supplied as appropriate in context. Other unattributed parenthetical notes within the body of an item originate with the source. Times within items are as given by source.

The contents of this publication in no way represent the policies, views or attitudes of the U.S. Government.

APPROVED FOR RELEASE: 2007/02/08: CIA-RDP82-00850R000100010054-0

BIBLIOGRAPHIC DATA SHEET	1. Report No. JPRS L/ 8247	2.	3. Recipient's Accession No.
4. Title and Subtitle TRANSLATIONS ON USSR SCIENCE AND TECHNOLOGY - PHYSICAL SCIENCES AND TECHNOLOGY, (FOUO 6/79)			5. Report Date 29 January 1979 6.
7. Author(s)			8. Performing Organization Rept. No.
9. Performing Organization Name and Address Joint Publications Research Service 1000 North Glebe Road Arlington, Virginia 22201			10. Project/Task/Work Unit No. 11. Contract/Grant No.
12. Sponsoring Organization Name and Address As above			13. Type of Report & Period Covered 14.

15. Supplementary Notes

16. Abstracts

The report contains information on aeronautics; astronomy and astrophysics; atmospheric sciences; chemistry; earth sciences and oceanography; electronics and electrical engineering; energy conversion; materials; mathematical sciences; cybernetics, computers; mechanical, industrial, civil, and marine engineering; methods and equipment; missile technology; navigation, communications, detection, and countermeasures, nuclear science and technology; ordnance; physics; propulsion and fuels; space technology; and scientists and scientific organization in the physical sciences.

17. Key Words and Document Analysis. 17a. Descriptors

USSR
Aeronautics
Astronomy
Astrophysics
Atmospheric Sciences
Chemistry
Computers
Cybernetics
Earth Sciences
Oceanography
Electronics
Electrical Engineering
Energy Conversion
Materials
Mathematics
Mechanical Engineering
Civil Engineering
Industrial Engineering
Marine Engineering
Methods
Equipment
Missile Technology
Navigation and Communications
Detection and Countermeasures
Nuclear Science and Technology
Ordnance
Physics
Propulsion and Fuels
Space Technology

17b. Identifiers/Open-Ended Terms

17c. COSATI Field/Group 01,03,04,07,08,09,10,11,12,13,14,16,17,18,19,20,21,22

18. Availability Statement	19. Security Class (This Report)	21. No. of Pages
For Official Use Only. Limited Number of Copies Available From JPRS	UNCLASSIFIED	55
	20. Security Class (This Page) UNCLASSIFIED	22. Price

FORM NTIS-35 (REV. 3-72) THIS FORM MAY BE REPRODUCED USCOMM-DC 14952-P72

JPRS L/8247

29 January 1979

TRANSLATIONS ON USSR SCIENCE AND TECHNOLOGY
PHYSICAL SCIENCES AND TECHNOLOGY

(FOUO 6/79)

CONTENTS PAGE

CONTENTS (Continued) Page

ELECTRONICS AND ELECTRICAL ENGINEERING

UDC 621.373.51; 621.372.837.4

THE RESONANCE ARRAY AND ITS APPLICATION TO THE DESIGN OF SOLID-STATE MICROWAVE DEVICES

Kiev IVUZ RADIOELEKTRONIKA in Russian Vol 21 No 10, Oct 78 pp 24-31

[Article by I.V. Lebedev and V.G. Alybin, manuscript received 23 Nov 77]

[Text] A new variant of a waveguide-rod structure is described, which possesses parallel and series resonances and provides for the efficient connection of a large number of semiconductor oscillator, switching or rectifier diodes. A design example of a multidiode microwave switch and limiter is treated.

Introduction

In the majority of modern waveguide oscillators, amplifiers, switchers and limiters, the microwave diode is positioned transverse to the waveguide, parallel to the electrical field vector, or inserted in a break in the inner conductor of the coaxial line, and coupled to the waveguide in one fashion or another [1 - 4]. Waveguide detector heads, phase shifters, modulators, attenuators and other microwave devices using discrete solid state devices also have a similar structural design. The development of these designs is now taking the approach of not so much the synthesis of fundamentally new systems, as much as the path of analyzing and refining the parameters of the equivalent circuitry and improving the characteristics of the devices on this basis [5, 6]. In searching for new design solutions, there is a special need for multidiode microwave devices, which attract attention in connection with the problem of boosting the workign power. In the majority of cases, it is necessary to use splitters and bridges [7] in multidiode devices, something which leads to an increase in the size and weight, or it is necessary to employ power addition using the principle of active diaphragms [8], something which does not provide for the requisite heat sinking and is inadequately effective. A new variant of a waveguide-rod resonance structure is described in the following, which provides for the insertion of a large number of microwave diodes, where this structure does not have the drawbacks indicated. The electrodynamic properties of this system are of independent interest, and in a number of cases, permit a significant improvement in the microwave parameters and characteristics of the diode devices.

The Resonance Array in a Rectangular Waveguide

To illustrate the devices and the operational principle of the multidiode structure being described here, we shall initially turn to the conventional resonance metal diaphragm (window) in a waveguide with a rectangular cross-section using the H_{10} mode. Such a diaphragm (Figure 1a) can be described with sufficient precision by an equivalent circuit in the form of a parallel resonant circuit, which shunts the main transmission line, as shown in Figure 1b. The bandwidth characteristic of the losses induced L by the window (Figure 1c) has a minimum at a frequency f_0, which corresponds to parallel resonance and the practically complete passage of the signal through the waveguide. The quantity f_0, as is well known, depends on the relationship of the dimensions of the window l and b', and the cross-sectional dimensions of the waveguide a and b .

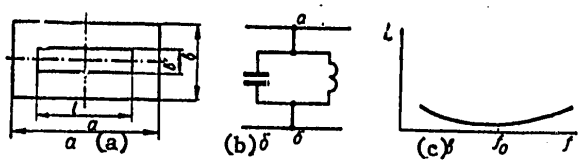

Figure 1. A resonance diaphragm in a rectangular waveguide (a), its equivalent circuit (b) and the shape of the bandwidth characteristic (c).

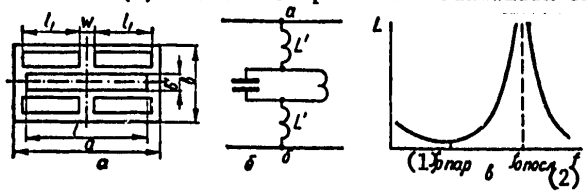

Figure 2. A diaphragm with four supplemental apertures (a) and its equivalent circuit and response with the parallel and series resonances (b, c).

Key: 1. f_0 parallel;
2. f_0 series.

We shall consider how the frequency response varies, which is shown in Figure 1c, where there are four supplemental openings of length l_1, which are depicted in Figure 2a, present in the plate of the diaphragm. If the dimension l_1 amounts to less than half of the free space wavelength, then each of the supplemental openings has an inductive conductivity. The equivalent circuit of the diaphragm takes on the form shown in Figure 2b, where L' are the equivalent inductances, determined by the dimensions of the supplemental slots and the width of the conducting strip w between them. As a result, there arises a second resonance at a frequency of $f_{0\ series}$, which no longer is of the parallel type, but is rather a series resonance (Figure 2c). This resonance, which corresponds to blocking of the waveguide, should be positioned at the higher frequency end with respect to the main parallel resonance $f_{0\ par}$, since the condition of series resonance of the main aperture

of the diaphragm with the inductance of the supplemental aperture is the capacitive nature of the impedance of the main opening.

It is not difficult to experimentally check the conclusions drawn here, by using a panoramic SWR meter to observe both attenuations of the broadband response of plane metal diaphragms which have fixed dimensions of the main opening l and b', and different dimensions of the supplemental openings. The frequency $f_{0\ par}$ practically does not change in this case, but the series resonance frequency $f_{0\ series}$ is controlled within a broad range and approaches the frequency $f_{0\ par}$ from the high frequency side with an increase in the dimension w.

In making a transition to the insertion of semiconductor diodes, just as in vacuum tube microwave electronics, it is necessary to take the approach of organically incorporating them into resonance structure. From this point of view, the diodes can be positioned in breaks in any of the conductors, which form the structure depicted in Figure 2a. However, the insertion of diodes in a break in the conductors, parallel to the electrical field vector in the waveguide, and which have a width w, is less expedient than in a break in the conductors parallel to the wide walls of the waveguide. This distinction is manifest particularly sharply when designing controlling class devices, for which the first of the variants cited here proves to be unacceptable. Thus, the insertion of diodes in a microwave structure can have the form shown in Figure 3a. Four oscillator, switching or rectifier diodes prove to be connected in pairs through the narrow walls of the waveguide. The conductors which are the extension of the diodes can have the shape of rods, in the center of which metal pins are positioned, which are coupled to the wide walls of the waveguide. The dimension l, which determines the parallel resonance frequency, can differ in the general case from the wide sectional dimension of the waveguide a.

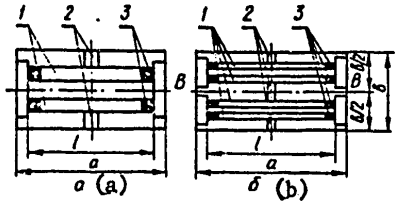

Figure 3. The connection of 4 and 8 semiconductor diodes:

1. Rods;
2. Pins;
3. Diodes.

The set of metal rods which are postioned parallel to the wide wall of the waveguide, with the diodes connected at their ends, and the metal pins, which connect the rods to the nearest wide walls of the waveguide, which possesses both parallel and series resonances, can be called a resonance array. In

following the principle described here, one can create not only 4-diode, but also 8-diode, 12-diode, 16-diode, etc. arrays. In particular, an 8-diode resonance array (Figure 3b) corresponds to the initial dual slot resonance window with eight supplemental openings, or what is the same thing, with two 4-diode resonance arrays in a waveguide of half the height, b/2, with respect to the plane of symmetry BB. The increase in the number of diodes is primarily limited by the narrow cross-sectional dimension of the waveguide and the sizes of the diode packages. To further the number of diodes, one can take the approach of using unpackaged diodes or waveguides with a non-standard cross-section with an increased height, including multimode waveguides.

The minimum possible number of diodes, inserted using the principle described here, is two. Such a configuration corresponds to a symmetrical division of the 4-diode array in awaveguide of twice the height of the conducting plane, arranged on analogy with the AA plane in Figure 3a, which can be positioned between two rods of a waveguide parallel to the wide wall, as shown by the dashed and dotted line in Figure 3a.

A general feature of the arrays treated in [9] is the positioning of the axes of the diodes and the rods connected to them perpendicular to the lines of the electrical field in the waveguide. It is not difficult to see that with such a configuration, the rods with the diodes prove to be decoupled with respect to the H_{10} mode field. The part of the devices exciting the rods is played by the pins, which connect the center taps of the rod to the opposite wide walls of the waveguide, or when the number of diodes is more than four, which connect the centers of the center rods in pairs. The same pins perpendicular to the wide walls of the waveguide are used to feed the suplly voltages in the case of oscillator and controlled diodes, or to complete the direct current circuit for the diodes in limiters and rectifiers.

The Equivalent Circuit of the Array

The direct utilization of the equaivalent circuit depicted in Figure 2b in calculations encounters difficulties in view of the fact that the length of the rods is commensurate with a half wavelength and there is a stronly pronounced variation in the field over the length of the rods. We shall initially neglect the influence of the conducting planes (the wide walls of the waveguide) and the inhomogeneities produced by the diode packages. Then each pair of rods can be represented in the form of a symmetrical two-wire line, which is excited out of phase in the center with the pins as shown in Fiugre 4a. The characteristic impedance Z_{c1} of this line is determined by the cross-sectional dimensions of the rods and the spacing between them.

Treating the rods as a T mode two-wire line is facilated by the above mentioned absence of coupling between the field of the rod line and the field of the H_{10} wave in the waveguide.

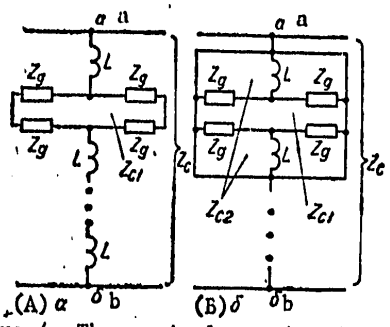

Figure 4. The equivalent circuits of a multidiode, resonance array.

The characteristic impedance of the line into which the array is connected is designated as Z_c in Figure 4a, i.e., the equivalent impedance of the main waveguide Z_e, where l is the total length of the rods between the end faces of the metal projection, including the length of the diodes. The total impedance of one diode is designated as Z_d.

The impedances of each pair of diodes, connected at the end of the two-wire line, proved to be connected in series with respect to the high frequency, although with respect to direct current, these diodes can have a parallel configuration. We will note that the series RF connection of the diodes is here achieved automatically without the physical superpostion of semiconductor structures and without degrading the conditions for heat removal from each of the diodes. The overall capacitance of each pair of diodes proves to be half the real capacitance of one diode, a circumstance which plays an important part and is an additional advantage of a resonance array over hitherto existing diode heads.

A further refinement of the equivalent circuit is shown in Figure 4b, where sections of conductor type lines above the conducting plane are taken into account, where they are formed by the rods and the wide walls of the waveguide close to them. Taking these lines into account, which have a characteristic impedance of Z_{c2}, is justified for the case of small spacings between the rods anc wide walls of the waveguides (see below).

Depending on the purpose of the device in which the resonance array is employed, one or both of the resonances shown in Figure 2c can be used. In this respect, a typical case is that of a switching resonance array, for which it is necessary to realize two operational modes: that of blocking and passing the signal in the main waveguide channel in the same passband.

A Multidiode Switcher and Limiter

We shall use the equivalent circuit shown in Figure 4a, and we shall treat the switching and limiting diodes only in two limiting states. In the first state, which corresponds to direct current flow through the diode, $Z_d \to 0$. In the second state (high impedance), the quantity Z_d is primarily determined by the capacitance of the diode C. Then, in the microwave signal cutoff mode, i.e., in the radar transmit mode, in the case of the "forward" circuit of the switcher, the input impedance of the array at the points ab in Figure 4 proves to be equal to

$$Z_{ab1} = jN\left(4\pi fL + \frac{Z_{c1}}{2}\operatorname{tg}\frac{\pi fl}{c}\right) = jX_{ab1}, \qquad (2)$$

where L is the inductance of the pin; c is the speed of light in free space and N is the number rod pairs.

In view of the purely reactive nature of the impedance Z_{ab1}, the decoupling which is provided in the signal cutoff mode amounts to:

$$L_{\text{decoupling}} = L_{\text{разв}} = 10 \lg \left[1 + \left(\frac{Z_c}{2X_{ab}} \right)^2 \right]. \quad (3)$$

A decoupling maximum is achieved at the series resonance frequency $f_{0\ \text{series}}$ when $X_{ab1} = 0$, from which:

$$\operatorname{tg} \frac{\pi f_{0\ \text{посл}}\, l}{c} = -\frac{8\pi f_{0\ \text{посл}}\, L}{Z_{c1}}. \quad (4)$$

In the microwave signal passage mode taking into account the series connection of the diode capacitances in pairs, we obtain the input impedance of the array with respect to the points ab in Figure 4a:

$$Z_{ab2} = jN \left(4\pi f L + \frac{Z_{c1}}{2} \frac{Z_{c1} \operatorname{tg} \frac{\pi f l}{c} - \frac{1}{\pi f C}}{Z_{c1} + \frac{1}{\pi f C} \operatorname{tg} \frac{\pi f l}{c}} \right) = jX_{ab2}. \quad (5)$$

The subscripts 1 and 2 in expressions (2) - (5) and the following correspond to the blocking and passage modes respectively, i.e., to the radar transmit and receive modes.

The losses introduced on receive, L_{intro}, are determined by expression (3) where X_{ab2} is substituted for X_{ab1}. In the approximation adopted here (without taking the active losses into account), the quantity L_{intro} should be equal to zero at the parallel resonance frequency $f_{0\ \text{par}}$, for which $X_{ab2} = \infty$. Taking (5) into account, we obtain

$$\tan (\pi f_{0\ \text{series}} l/c) = \pi f_{0\ \text{series}}\, C Z_{ci} \quad (6)$$

The condition for normal operation of the switcher and limiter is the colocation of the frequencies $f_{0\ \text{par}}$ and $f_{0\ \text{series}}$ at a specified center frequency f_0. From this, using (5) and (6), one can determine the requisite inductance L of the pins which connect the rods to the wide walls of the waveguide

$$L = \frac{C Z_{c1}^2}{8}. \quad (7)$$

As can be seen from (7), with a decrease in the diode capacitance C or the characteristic impedance of the rod line Z_{c1}, it is necessary to reduce the inductance of the pin L. For this purpose, for example, one can make use of the reduction in the existing length of the pins by means of choke cylinders, introduced into the waveguide [10]. The evaluation based on equation (7) shows that for typical values of C = 0.5 — 1 pF and Z_{c1} = 100 — 150 ohms,

the quantity L should fall in a range of 0.6 -- 2.8 nHy. The length l of the rods which provides for the specified value of f_0 can be found by means of (6):

$$l = \frac{c}{\pi f_0} \operatorname{arctg}(-\pi f_0 C Z_{c1}). \quad (8)$$

The quantity l always proves to be somewhat greaer than half of the resonance wavelength in free space, equal to $\lambda_0 = c/f_0$. With a decrease in the capacitance, the length l should be increased, a maximum where $C \to 0$, $l \to \lambda$. The length l can be both somewhat smaller and somewhat greater than the wide dimension of the waveguide section a, since usually $a \approx (0.7 -- 0.8)\lambda$.

In practice, it is convenient to position the diodes in pairs on metal inserts, as shown schematically in Figure 3.

The choice of the characteristic impedance of the rod line Z_{c1} requires special attention. An increase in Z_{c1} following the corresponding correction of the quantities L and l while observing f_0 = const., leads to an expansion of the bandwidth in the receive (passage) mode and simultaneously to a narrowing of the bandwidth in the transmit (signal blocking) mode. It usually necessary to specify the minimum permissible amount of decoupling in the transmit mode, L_{10}, at the edges of the band and the maximum permissible amount of introduced losses L_{20}. Typical values of L_{10} and L_{20} are 15 -- 20 dB and 0.5 -- 1.0 dB respectively. Assuming the indicated values of L_{10} and L_{20}, one can solve the two transcendental equations for $L_{dec} = L_{10}$ and $L_{intro} = L_{20}$ by means of equations of type (3). The roots of these equations which are closest to the frequency f_0 yield the boundary frequencies of the resultant passband in the receive mode Δf_2 and the bandwidth in the transmit mode Δf_1.

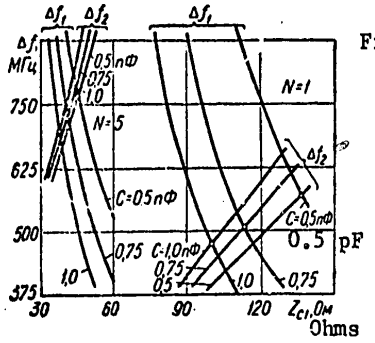

Figure 5. The bandwidth in the two operational modes as a function of the characteristic impedance of rod lines for 4-diode and 20-diode switchers and limiters:

a = 28.5 mm;
b = 12.6 mm;
L_{10} = 20 dB;
L_{20} = 0.5 dB.

The typical depedence of the bandwidth Δf_1 and Δf_2 on the characteristic impedance Z_{c1} is shown in Figure 5 for three values of diode capacitance C in the centimeter band for the case of 4-diode (N = 1) and 20-diode (N = 5) arrays. The intersection of the Δf_1 and Δf_2 curves yields the quantity Z_{c1}, which satisfies not only the above mentioned colocation of the frequencies $f_{0\ series} = f_{0\ par} = f_0$, but also the coincidence (equality) of the bandwidth

in both working modes: $\Delta f_1 = \Delta f_2$*. As can be seen from the Figure, with a decrease in diode capacitance or with an increase in the number of rods in the array, and correspondingly the number of diodes, a notable expansion of the working bandwidth is achieved. The requisite quantity Z_{c1} in this case decreases with an increase in N.

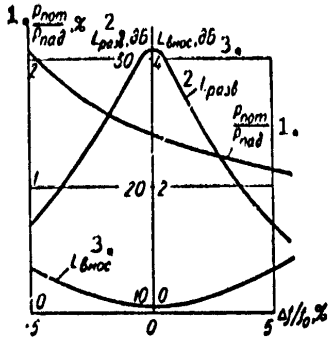

Figure 6. The band characteristics of the decoupling of the introduced losses and dissipated power for a 4-diode switching array:

a = 28.5 mm;
b = 12.6 mm;
R_{d1} = 2 ohms;
R_{d2} = 0.3 ohms;
C = 0.5 pF.

Key: 1. P_{diss}/P_{inc}, percent;
2. $L_{decoupling}$, dB;
3. L_{intro}, dB.

Another important improvement in the characteristics of switches and limiters is also achieved with an increase in the number of diodes: a reduction in the electrical load which is characterized by the power dissipated in one diode, and a sharp increase in the maximum power of the incident wave. The calculation of the electrical load can be carried out using the same equivalent circuit (Figure 4a), taking into account the finite amount of resistance of the diode R_{d1}. A typical variation in the power P_{dis}, dissipated in one diode, referenced to the power of the incident wave, P_{inc}, is shown in Figure 6 for a 4-diode array. Also derived there are the calculated bandwidth characteristics of the introduced losses and decoupling, taking into account the finite values of the diode resistances in the transmit mode R_{d1} and in the receive mode R_{d2}. As can be seen from these curves, the maximum of the dissipated power can fall outside the range of the working bandwidth on the low frequency side.

The Influence of the Waveguide Walls

A more precise equivalent cirucit, which is depicted in Figure 4b, permits taking into account the influence of the wide walls of the waveguide on the characteristics and parameters of the resonance array in a first approximation. The input impedance of the switching or limiting array at points ab is described by the general equation in this case:

* Due to the small asymmetry in the bandwidth characteristics, there exists a certain divergence of the boundary frequencies in the transmit and receive modes, even when $\Delta f_1 = \Delta f_2$. This divergence can neglected in a first approximation.

$$[Z_д = Z_d]. \quad Z_{об1.э} = \frac{Z_{c1}}{2}\frac{Z_д + j\frac{Z_{c1}}{2}\operatorname{tg}\frac{\pi f l}{c}}{\frac{Z_{c1}}{2} + jZ_д \operatorname{tg}\frac{\pi f l}{c}} + \frac{j2\pi f L Z_{c2}\left(Z_д + jZ_{c2}\operatorname{tg}\frac{\pi f l}{c}\right)}{j2\pi f L(Z_{c2} + jZ_д) + \frac{Z_{c2}}{2}\left(Z_д + jZ_{c2}\operatorname{tg}\frac{\pi f l}{c}\right)}. \tag{9}$$

Here Z_{c2} is the characteristic impedance of the conductor type line above ground, which is formed by the wide wall of the waveguide and the array rod which is closest to it.

By again applying the condition for the colocation of the decoupling maximum in the transmit mode and the minimum of the introduced losses in the receive mode, one can derive an expression which determines the requisite inductance of a pin:

$$L = \frac{CZ_{c1}^2}{4\left(2 + \frac{Z_{c1}}{Z_{c2}}\right)}. \tag{10}$$

When $Z_{c2} \to \infty$, (10) transforms into (7). The length of the rods in the approximation considered here is, as before, determined by expression (8).

Calculations show that the influence of line sections with a characteristic impedance of Z_{c2} have the most pronounced effect on the amount of the power dissipated in the diodes, and on the frequency characteristics of the entire array in the transmit mode. It is interesting to note that the frequency response of the power dissipated in the diode, with a reduction in the impedance Z_{c2}, can cease to be a decaying value with an increase in frequency. The rise in the power dissipated in the diodes at the high frequency edge of the band is due to the parallel resonance between the inductance of the pins and the input impedance of the conductor-above-ground type line. There is simultaneously a certain narrowing of the bandwidth of the array in the transmit mode.

The influence of the sections of lines of the conductor above a conducting plane type is also manifest in another fashion. The difference in the inductances of the pins, perpendicular to the wide walls of the waveguide, has extremely little effect on the band response characteristics of decoupling and introduced losses, but at small values of Z_{c2}, leads to imbalance in the electrical load of the diodes, connected at the ends of the different rods. For this reason, when aligning an array by means of moving choke devices, which provide for a variation in the frequency f_0 series, it is desirable to monitor the symmetry of the electrical load, which can be accomplished in practice by a number of methods. The possibility of adjusting and monitoring the power dissipated by the diodes permits compensating for the scatter in the production parameters of the diodes and in the array as a whole.

Conclusion

The analysis and design of other applications of a resonant array can be carried out in a similar manner: for cases of pwer addition for oscillators

and amplifiers using IMPATT diodes and Gunn diodes, as well as for the case of multidiode microwave rectifiers, etc. A number of questions of the operation of such devices is of independent interest.

BIBLIOGRAPHY

1. Eisenhart R.L., "Understanding the Waveguide Diode Mount", IEEE GMTT Int. Microwave Symp., Arlington Heights, Dig. Techn. Pap., N.Y., 1972, 1954.

2. Lebedev I.V., "Nekotoryye problemy gazorazryadnykh i tverdotel'nykh SVCh pereklyuchateley" ["Some Problems of Gas Discharge and Solid State Microwave Switchers"], IZV. VUZOV - RADIOELEKTRONIKA [PROCEEDINGS OF THE HIGHER EDUCATIONAL INSTITUTES - RADIO ELECTRONICS], 1973, 16, No 10, p 41.

3. Liberman L.S., Sestroretskiy B.V., Shpirt V.A., Yakuben' L.M., "Poluprovodnikovyye diody dlya upravleniya moshchnost'yu" ["Semiconductor Diodes for Power Control"], RADIOTEKHNIKA [RADIO ENGINEERING], 1972, 27, No 5, p 9.

4. Kurokawa K., "The Single-Cavity Multiple Diode Oscillator", IEEE TRANS., 1971, MTT-19, No 10, p 793.

5. Williamson A.G., Otto D.V., "Analysis of a Waveguide Mounting Structure", PIEEE, 1973, 34, No 3, p 95.

6. Bugayev V.Ya., Rapoport G.N., "Ekvivalentnaya skhema volnovodno-koaksial'nogo T-sochleneniya" ["An Equivalent Circuit of a Waveguide to Coaxial T-Coupling"], IZV. VUZOV - RADIOELEKTRONIKA, 1977, 20, No 2, p 95.

7. Kuno H.T., Englisch D.L., "Millimeterwave IMPATT Power Amplifier Combiner", IEEE TRANS., 1976, MTT-24, No 11, p 758.

8. Hefni I.E., "Microwave Semiconductor Device Mount", US Patent, Cl. 333-83, No 345 2305, Claim 28 Feb 67, published 24 Jun 69.

9. Lebedev I.V., Alybin V.G., "Ustroystvo slozheniya moshchnostey sverkhvysokochastotnykh priborov" ["Microwave Device Power Combiner"], Patent No 566297, BYULLETEN' IZOBRETENIY [BULLETIN OF INVENTIONS], 1977, No 27.

10. Baker T.H.B., "Semiconductor Diode Waveguide Switch", ELECTRONIC TECHNOLOGY, 1961, 38, No 8, p 300.

11. Lebedev I.V., Alybin V.G., Ashkenazi D.Ya., Belyayev V.P., "Moshchnyy mnogodiodnyy volnovodnyy pereklyuchatel'" ["A High Power Multidiode Waveguide Switch"], ELEKTRONNAYA TEKHNIKA [ELECTRONIC ENGINEERING], Seriya 1, ELEKTRONIKA SVCh [MICROWAVE ELECTRONICS], 1977, No 9.

8225
CSO:1870

ELECTRONICS AND ELECTRICAL ENGINEERING

UDC 621.372.825.4

ESTIMATING THE PROPERTIES OF PERIODIC STRUCTURES FOR MULTIBEAM MICROWAVE DEVICES

Kiev IVUZ RADIOELEKTRONIKA in Russian Vol 21 No 10, Oct 78 pp 90-95

[Article by F.F. Dubrovka, V.I. Naydenko and A.A. Sakalosh, manuscript received 25 Nov 77]

[Text] The expediency of using a chain of coupled ring resonators in multibeam, type O microwave devices is demonstrated. The concept of a generalized coupling impedance is introduced, based on which the properties of retarding systems are evaluated for the type where a chain of ring resonators and a chain of inductively coupled resonators are used as the structures for multibeam microwave devices.

The refinement of radio engineering equipment requires the design of high power, type O microwave devices which have low power supply voltages voltages. One of the promising approaches to the solution of this problem is that of going over to multibeam devices, in which by virtue of increasing the interaction region in the transverse direction, one can boost the perveance by tens of times, and thereby, obtain the requisite power levels at comparatively low voltages.

Of all of the well-known retarding systems, a chain of inductively coupled resonators, which is called a *stopped waveguide* in the following, has become widespread in high power type O devices. This is due to its outstanding electrodynamic, production technology and thermal characteristics. It is only natural that a stopped waveguide was used by the designers of multibeam devices. The properties of other periodic structures were not investigated as applicable to their use in multibeam devices.

It is expedient to use a chain of coupled ring resonators as the retarding system for multibeam type O microwave devices, where the central rod in this chain, which shorts out the diaphragm stops, displaces the longitudinal electrical field from the central region to the peripheral region, and thereby increases the region of effective interaction of the field with the electron flows.

Described below are the properties of fields in a chain of coupled ring resonators. A comparison is made on the basis of the introduced concept of a generalized coupling impedance between the properties of this structure and of a stopped waveguide from the viewpoint of their application in multibeam type O microwave devices.

It is well known [1, 2] that with a phase shift through a period, $\phi \to 0$, the properties of retarding systems of the coupled resonator chain type become closer to the properties of a system of uncoupled resonators the smaller the thickness of the stops (for the case of zero thickness of the stops, the cut-off wavelength λ corresponding to $\phi = 0$, is precisely equal to the resonance wavelength of the uncoupled resonators). For this reason, a good initial approximation for fields close to $\phi = 0$ will be the fields of an isolated resonator. For a ring resonator with an outer cylinder radius of b and an inner radius of the (center, coaxial) metal rod c, the longitudinal electrical fields, where the number of variations in azimuth is m, are represented in the form [3]:

$$\begin{aligned} E_z &= A\left[J_m(kr)N_m(kb) - J_m(kb)N_m(kr)\right]\sin m\varphi, \\ H_\varphi &= -A\frac{i\omega\varepsilon}{k}\left[J'_m(kr)N_m(kb) - J_m(kb)N'_m(kr)\right]\sin m\varphi, \\ H_r &= A\frac{i\omega\varepsilon m}{k^2 r}\left[J_m(kr)N_m(kb) - J_m(kb)N_m(kr)\right]\cos m\varphi. \end{aligned} \tag{1}$$

here $J_m(x)$, $N_m(x)$, $J'_m(x)$ and $N'_m(x)$ are m order Bessel functions of the first and second kind and their derivatives with respect to the argument x; $k = 2\pi/\lambda$ is the wave number.

Formulas (1) represent a field which has no variations along the axis of the resonator.

The resonance frequencies of the E_{mn0} modes of a ring resonator are found as the roots of the equation

$$J_m(kc)N_m(kb) - J_m(kb)N_m(kc) = 0. \tag{2}$$

We will note that the fields of a stopped waveguide with infinitely thin diaphragm stops where $\phi = 0$ differ from the fields of (1) by the substitution of the Bessel function $J_m(kr)$ (or $J'_m(kr)$ for the H subscript ϕ component) for the expressions in the square brackets, while the resonance frequencies are found as the roots of the equation

$$J_m(kb) = 0. \tag{3}$$

The distributions of the electrical field E_z and the magnetic field H_ϕ intensities over the radius for different ratios of the inner and outer conductor radii c/b are given in Figure 1a, b. The solid lines show the distribution of the fields in a system without an inner conductor (c/b = 0), the dashed lines are for a system with c/b = 0.02, and the dashed and dotted lines

are for a system with c/b = 0.4. The number of variations of the fields over the azimuth m amounted to 0.1 and 2 (the corresponding numbers on the curves).

As can be seen from Figure 1, the introduction of a center conductor exerts the greatest influence on the azimuthally homogeneous fields (m = 0); with an increase in m, the influence of the center conductor falls off. With an increase in the radius of the center conductor c, the maximum of the field E_z is shifted into the region of greater values of r/b, and the distributions of the fields with different values of m come closer together.

The distribution over the radius of the difference in the densities of the magnetic and electrical energy $\mu|H_\phi|^2 - \varepsilon|E_z|^2 = \Delta W$ is shown in Figure 2. The parameters c/b and m and the designations of the curves are the same as in Figure 1. As can be seen from Figure 2, with the introduction of a rod ΔW of the azimuthally homogeneous type of oscillations changes the most sharply: when c/b = 0, the electrica field energy is concentrated in the region of small values of r/b; when $c/b \neq 0$, the energy of the magnetic field is concentrated in the same region. Figure 2, in particular, determines the regions which are expediently used to realize magnetic coupling between the resonators. For example, when c/b = 0, it is expedient to cut the coupling slots in the diaphragm stops in the region of ratios of r/b of 0.6 — 1 for m = 0; 0.77 — 1 for m = 1, and 0.83 — 1 for m = 2.

Where a center conductor is present, there are two regions in which the magnetic field energy predominates. This permits magnetic coupling not only in the peripheral part of the ring resonator, but also in the central part.

The more sharply the fields vary, the more strongly the resonance wavelength λ changes, something which is evidenced by the curves shown in Figure 3. Here, the ratio of the wavelength corresponding to $\phi = 0$ to the diameter of the outer conductor 2b is plotted along the ordinate. The intersection with the ordinate axis marks the point corresponding to λ of a stopped waveguide. It can be seen that with an increase in c, the system becomes even more short wave and the curves corresponding to various values of m come closer together. This complicates the elimination of interfering modes, something which should be taken into account when using such systems in electronic devices.

One of the main quantities which is used the most frequently as the characteristic of retarding systems is the coupling impedance n of the spatial harmonic which interacts with the electron flow [1, 2].

$$R_n = \frac{|E_z|^2}{2\beta_n^2 P}.$$

However, it turns out that the quantity R_n is an incomplete characteristic for a retarding system, especially in the case where it is used in multibeam devices. In fact, one of the main electrical parameters in the theory of type O devices is the Pearce gain parameter [4] $C = (R_n I/4U)^{1/3}$, and is

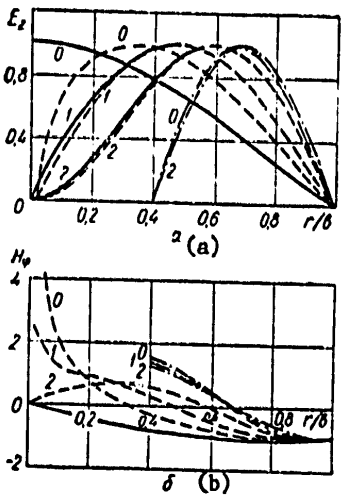

Figure 1.

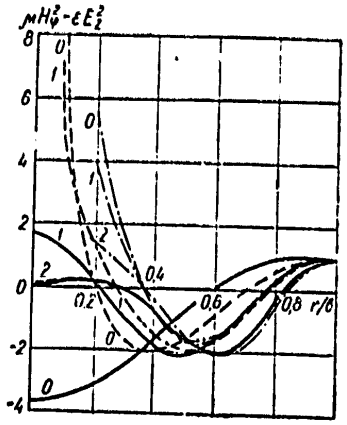

Figure 2.

is determined not only by the coupling resistance R_n of the working spatial harmonic, but also by the current I and the voltage U of the beam. Neglecting relativistic effects, $U \approx n_n^{-2}$ [4], where n_n is the delay of the n-th working spatial harmonic. Taking this coupling into account, it is clear that the properties of a retarding system are more completely characterized by the parameter $R_n n_n^2$. The beam current $I = j_k S_k = j_c S_c$ is limited in the cathode region by the emission current density from the cathode j_k and the area of the cathode S_k, while in the interaction region, the current density in the channel of the system j_c and the area of the channel cross-section S_c is limited by the power engineering capabilities of the electron-optical system. It is known that the greater S_c is, the less the coupling resistance R_n is. Thus, the parameter which most completely characterizes the system at a specified wavelength from the power engineering viewpoint is the product $R_n n_n^2 k_\pi$, where k_π is the ratio of the area occupied by the beam to any characteristic area. We will note that for a more precise analysis, it would be necessary to include in the channel area also the area in which the longitudinal electrical field interacting with the beam is concentrated, i.e., also include the area occupied by the connecting sleeves in the cross-secional area of the channel S_c. However, the cross-sectional area of the channel is usually considerably greater than the area taken up by the coupling sleeves, and it is sufficient to just consider S_c.

Further, the band properties of the retarding system are characterized by the group velocity v_{rp} [v_{gr}] or by the group delay $n_{rp} = [n_{gr}] = c/v_{gr}$ (where c is the velocity of light in a vacuum), and the greater n_{gr}, the greater R_n, the smaller the working bandwidth of the device.

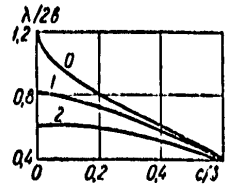

Figure 3.

Thus, we arrive at a generalized coupling resistance, a parameter which most completely characterizes a retarding system:

$$\frac{R_n}{n_{гр}} n_n^2 k_n, \qquad (4)$$

which in the international system of units has the dimensions of ohms.

We will note that parameter (4), in contrast to R_n, also characterizes the systems at the edges of the passband, and in particular, it is also suited as a characteristic of resonators, while R_n at the edges of the passband for any system tends to ∞. Moreover, the quantities measured in the completely matched mode (the standing waves) are specifically proportional to $(R_n/n_{gr})n_n^2$. This also makes parameter (4) convenient in experimental studies of retarding systems.

By returning to a system of a chain of coupled ring resonators, we find

$$\frac{R_0}{n_{гр}} n_0^2 = \frac{30}{(kb)^2} \delta_m \frac{|E_z|^2}{|H_\varphi(kb)|^2 - \left(\frac{c}{b}\right)^2 |H_\varphi(kc)|^2}, \qquad (5)$$

where $\delta_m = 1$ when $m = 0$ and $\delta_m = 2$ when $m \neq 0$; $H_\phi(kb)$ and $H_\phi(kc)$ are the values of the H_ϕ component of the magnetic field (1) when $r = b$ and $r = c$; kb [$kc = kb\ (c/b)$] is determined from equation (2). Taken into account in (5) is the coupling $P = v_{gr}W/L$, where W is the energy stored over a period of the system L.

In the right hand side of (5), $|E_z|^2$ depends on r and ϕ, and for this reason, $(R_0/n_{gr})n_0^2$ is also a function of r and ϕ. Specifically, one can choose such values of r and ϕ that $|E_z|$ is either maximum or $|E_z|$ is averaged over the cross-section of the beam. Given below are values of $(R_0/n_{gr})n_0^2$ at the point where $|E_z|$ has a maximum.

The results of calculating $(R_0/n_{gr})n_0^2$ as a function of c/b for $m = 0$ are shown in Figure 4 by the solid line. When $c/b = 0$, the quantity $(R_0/n_{gr})n_0^2 = 38.5$ ohms. With an increase in the diameter of the inner conductor, $(R_0/n_{gr})n_0^2$ falls off. For example, when $c/b = 0.1$, $(R_0/n_{gr})n_0^2 = 12.2$ ohms, i.e., it has fallen off to practically a third of its former value. But with the introduction of an inner conductor, as seen in Figure 1, the area which can be occupied by the beam is changed substantially. In other words, a considerably greater current I can be introduced in a system with a central inner conductor. For this reason, it is also necessary to take into account the area coefficient k_n.

The efficient operation of multibeam devices can be achieved where alllof the beams are located in an RF field of close intensity.

The level of the permissible variation in the electric field intensity is determined by the area which can be occupied by the beam. For example, as

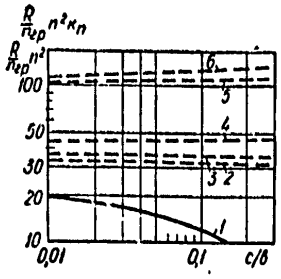

Figure 4.

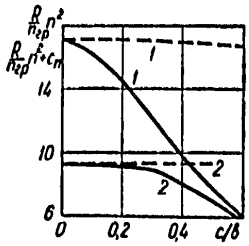

Figure 5.

follows from Figure 1, if vertical line $|E_z|^2$ is taken at the 0.81 level (i.e., $|E_z|$ at a level of 0.9), then the area which can be occupied by the beam in a system with c/b = 0 amounts to about 6.5% of the cross-sectional area of the system. If we limit ourselves to the same level of variation in $|E_z|^2$, but use a system with a center inner conductor with c/b = 0.1, then the area which can be occupied by the beam will be 9.6 times greater (the diameter 2b increases, as can be seen from Figure 3, by 1.37 times for the case of a constant λ).

For a comparative estimate of a stopped waveguide and a system of a chain of coupled ring resonators, the parameter k_π is determined from the formula

where $S_\alpha|_{c/b>0}$ is the area which can be occupied by the beam if a drop in $|E_z|^2$ down to a level of α is permitted in the chain of coupled ring resonators, and $S_\alpha|_{c/b=0}$ is the same, but in a stopped waveguide.

The results of calculating $R_0 n_0^2 k_\pi / n_{gr}$ for azimuthally homogeneous fields is shown in Figure 4 by the dashed lines, where curve 2 corresponds to an α of 0.16; 3 corresponds to a level of 0.25; 4 corresponds to a level of 0.49; 5 to a level of 0.81 and 6 to a level of 0.9. As can be seen from Figure 4, with an increase in c/b and the level α, the quantity $R_0 n_0^2 k_\pi / n_{gr}$ increases, reaching a level of about 150 ohms. We will note that this same quantity $R_0 n_0^2 k_\pi / n_{gr}$ for a system without a center conductor ($k_\pi = 1$) is equal to 38.5 ohms. Thus, for the permissible level of reduction in $|E_z|^2 = 0.81$, the parameter $R_0 n_0^2 k_\pi / n_{gr}$ of a system with a center conductor is three to four times greater than the same parameter of a stopped waveguide.

These same curves for azimuthally inhomogeneous oscillations where m = 1 and m = 2 are shown in Figure 5 (the designations are the same as in Figure 4). With an increase in c/b, the quantity $R_0 n_0^2 / n_{gr}$ falls off, while the quantity $R_0 n_0^2 k_\pi / n_{gr}$ remains approximately constant for both m = 1 and for m = 2.

The comparison given here for the properties of systems where a chain of coupled ring resonators and a stopped waveguide are used applies to a phase

shift of $\phi = 0$. Numerous experimental investigations carried out on various retarding systems have shown that the quantity $R_{on}Q/n_{gr}$, taken at the surface of the transit channel, in the first place, varies comparatively weakly in the passband, and in the second place, something which is especially important, with a change in the geometry of the system is shifted practically parallel to itself. This permits the extension of the results obtained to the entire passband, as well as a comparison of different systems in the passband which have the requisite information only at one point in the passband, for example, at the point $\phi = 0$, as was done above. Consequently, it is obvious that it is expedient to make practical use of the introduced genralized coupling resistance, a quantity which most completely characterizes a retarding system.

Thus, this paper has studied the properties of fields in a chain of coupled ring resonators where $\phi = 0$. The concept of a generalized coupling resistance has been introduced, and it has been shown that this quantity most completely characterizes the retarding system of multibeam devices. A comparison of the properties of a chain of coupled ring resonators and a stopped waveguide was made using the indicated quantity; it was demonstrated that a chain of ring resonators is to be prefered for type O multibeam microwave devices.

BIBLIOGRAPHY

1. Taranenko Z.I., Trokhimenko Ya.K., "Zamedlyayushchiye sistemy" ["Interactive Systems"], Kiev, Tekhnika Publishers, 1965.

2. Silin R.A., Sazonov V.P., "Zamedlyayushchiye sistemy" ["Interactive Systems"], Moscow, Sovetskoye Radio Publishers, 1966.

3. Nikol'skiy V.V., "Elektrodinamika i rasprostraneneiye radiovoln" ["Radio Wave Electrodynamics and Propagation"], Moscow, Nauka Publishers, 1973.

4. Gayduk V.I., Palatov K.I., Petrov D.M., "Fizicheskiye osnovy elektroniki SVCh" ["The Physical Principles of Microwave Electronics"], Moscow, Sovetskoye Radio Publishers, 1971.

8225
CSO:1870

GEOPHYSICS, ASTRONOMY AND SPACE

UDC 551.466.8

EXPERIMENTAL INVESTIGATION OF OSCILLATIONS OF A FREE SURFACE INDUCED BY INTERNAL WAVES

Moscow IZVESTIYA AKADEMII NAUK SSSR, FIZIKA ATMOSFERY I OKEANA in Russian Vol 14, No 11, 1978 pp 1216-1218

[Article by I. S. Dolina, S. A. Yermakov, V. V. Papko and Ye. N. Pelinovskiy, Institute of Applied Physics, USSR Academy of Sciences, submitted for publication 21 July 1977]

[Text] As is well known, internal waves in the ocean attain their maximum amplitudes in layers with the greatest density gradients. At the ocean surface the amplitudes of the internal waves are small (usually about several centimeters) and they are usually neglected [1]. However, as a result of increase in the accuracy of measurements of waves at the surface its displacements from internal waves can be registered. Surface oscillations caused by internal waves lead, for example, to oscillations of ice which were measured under natural conditions and which at least theoretically can serve as an indicator of internal waves [2, 3]. The influence of internal waves on surface displacements can also be of definite interest in an investigation of the spectrum of surface waves in the low-frequency range (frequencies of about 10^{-2}–10^{-4} s^{-1}), since internal waves evidently constitute one of the important sources of its formation. The theory of the spectra of surface waves induced by internal waves was examined in [4].

This communication is devoted to an experimental investigation of perturbations of the free surface of a stratified fluid caused by the internal waves propagating in it. The theoretical analysis is based on linear approximation formulas. As a result of an experimental investigation it was demonstrated that the dependence of surface displacement on wave frequency is described well by the formulas of linear theory, even after the appearance of nonlinear distortions of the wave form.

Surface perturbations from internal waves are determined (in the linear theory) by the structure of the normal mode, being a solution of the problem [1]

$$d^2W/dz^2+[\omega^{-2}N^2(z)-1]k^2W=0 \qquad (1)$$

[Equation (1) is written in the Boussinesq approximation.] with the boundary conditions: at the free surface

$$W+(\omega^2/gk^2)dW/dz=0, \quad z=0, \tag{2}$$

at the ocean floor

$$W=0, \quad z=H. \tag{3}$$

Here W(z) is the eigenfunction for the vertical velocity component; N(z) is the Väisälä frequency; H is ocean depth; ω and k are frequency and the horizontal wave number. Equations (1)-(3) describe both surface and internal waves. Surface waves with any N(z) have maximum displacements at the surface. The structure of the internal waves is essentially dependent on the N(z) profile. The maximum water level displacements in internal waves are attained at some horizons: however, near the surface the displacements are small so that frequently the boundary condition (2) is replaced by the simpler approximate "lid" condition.

$$W=0, \quad z=0, \tag{2a}$$

thereby excluding surface oscillations. Nevertheless, W(z), computed using (2a), can be employed for approximate computation of surface displacement (or vertical velocity) by means of equation (2), relating the small value W (z = 0) with the significant value $dW/dz \mid z = 0$; the latter is found from a solution of problem (2a). Such an algorithm for finding W (z = 0) is convenient for numerical computations since problem (2a) can be solved with a lesser accuracy, but for a shorter time, than problem (2).

Now we will cite the expressions used below, which are easily derived from (1)-(3), for displacement of the free surface ζ_{surf}, related to the maximum amplitude for the internal wave ζ_m, for two stratification models.

In a three-layer model with a linearly stratified middle layer (with the Väisälä frequency N)

$$\frac{\zeta_\pi}{\zeta_m} = -\frac{\omega^2}{gk}\left(\frac{N^2}{\omega^2}-1\right)^{1/2}\left[(\operatorname{ch} kh)^2+\left(\frac{N^2}{\omega^2}-1\right)(\operatorname{sh} kh)^2\right]^{-1/2}; \tag{4}$$

in a two-layer model (density drop $\Delta\rho$)

$$[\pi = \text{surf}] \qquad \frac{\zeta_\pi}{\zeta_m} = -\frac{\Delta\rho}{\rho}\frac{1}{k}\frac{\operatorname{sh} kh \operatorname{sh} k(H-h)}{\operatorname{sh} kH}, \tag{5}$$

where h is in both cases the depth of the upper homogeneous layer.

The dependences (4) and (5) for the mentioned stratification models were checked experimentally.

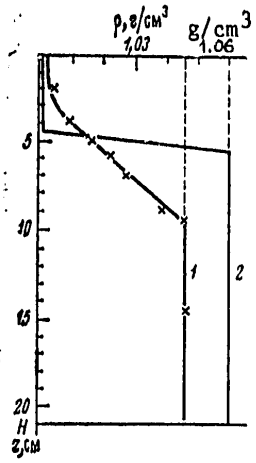

Fig. 2

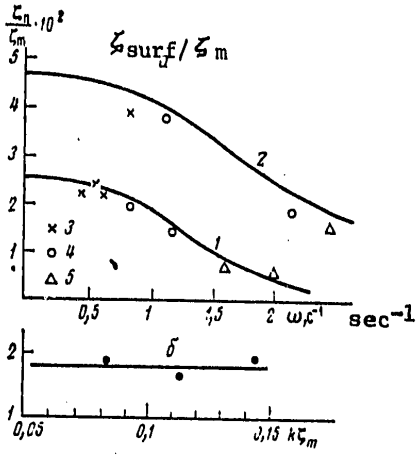

Fig. 4

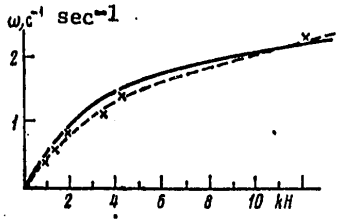

Fig. 3

Fig. 2. Dependence of fluid density ρ on depth z; 1) three-layer model with linearly stratified middle layer; 2) two-layer model

Fig. 3. Theoretical and experimental dispersion curve for three-layer model.

Fig. 4. Theoretical dependences and results of measurements of relative surface displacement ζ_{surf}/ζ_m: a) on frequency ω of internal wave (1 -- three-layer model, 2 -- two-layer model; points 3 -- slopes $k\zeta_m \sim 0.05$, 4 -- $k\zeta_m \sim 0.1$, 5 -- $k\zeta_m \sim 0.15$); b) on steepness $k\zeta_m$ of internal wave ($T \approx 6$ sec, three-layer model).

In order to carry out the experiment we used a plastic flume (3 x 0.5 x 0.2 m). A stable stratification was created by introducing salt solutions of different density into the flume. Internal waves were excited by a wave-generator, having the configuration of a wedge and driven into motion by a motor with an adjustable rate of rotation. In order to visualize internal waves in a region with a maximum density gradient we introduced a colored layer of fluid with a thickness 0.5-1 cm; however, when working with a two-layer model we colored the entire upper homogeneous layer (Fig. 1). The amplitudes of the internal waves (about a centimeter) and their lengths were measured using a scale grid plotted on the front wall of the bath. We note that similar methods for exciting and measuring internal waves within a fluid have been repeatedly described in the literature (for example, see [5]). However, no study has been made of the surface perturbations associated with internal waves.

In order to measure surface waves we fabricated sensors in the form of metal plates situated directly above the water surface. The capacitance between the plate and the water surface was the arm of a bridge circuit supplied current from an acoustic frequency generator. The signal fed from the bridge diagonal, after amplification, was fed to an oscillograph and an automatic recorder. The minimum surface displacements measured by the sensor were 10μm.

There was also simultaneous registry of the signals from two spaced sensors on an automatic recorder; this made it possible, using the phase difference, to measure the lengths of the surface waves. The latter is necessary in order to prove that the waves experimentally observed at the surface correspond to an internal wave (and are not a surface mode with the same frequency).

In the experiment the amplitudes of the internal waves varied in the range 0.5-1.5 cm, the wave length varied from 15 cm to a meter, the steepness from 10^{-1} to $5 \cdot 10^{-3}$. In this case the amplitudes at the surface were about 0.05-0.1 mm.

Below we give the measurement results for two types of stratification; a three-layer model with a linearly stratified middle layer ($N \approx 2.6\ s^{-1}$) and a model of a two-layer fluid ($\Delta\rho/\rho \approx 0.06$) (Fig. 2). Figure 3, for a three-layer model, shows the dependence of wave frequency ω at the fluid surface on the wave number k (dashed curve) ascertained experimentally using capacitive-type sensors. It can be seen that the experimental points agree well with the theoretical dispersion curve $\omega(k)$ for an internal wave of a lower mode, constructed using the known formulas of linear theory [6].

The experimental dependences of the relative amplitude of the internal wave at the surface ζ_{surf}/ζ_m on its frequency for two models are shown in Fig. 4,a. For both models there is a good agreement of experimental and theoretical curves (4), (5). It should be noted that with a wave

steepness of about 0.1 the wave configuration differs appreciably from a sine curve. The observed distortions of configuration of the internal waves are similar to those described in [5]. The relative displacement of the surface remained virtually the same as in a linear case (Fig. 4,b).

Thus, the experimental results cited above show that t' measured surface perturbations correspond to internal waves in a stratified fluid and are described well by the linear theory formulas.

BIBLIOGRAPHY

1. Phillips, O. M., DINAMIKA VERKHNEGO SLOYA OKEANA (Dynamics of the Upper Layer of the Ocean), "Mir," 1969.

2. Smirnov, V. N., "Ice Cover Oscillations Caused by Internal Waves in the Arctic Ocean," DOKLADY AN SSSR (Reports of the USSR Academy of Sciences), 206, No 5, 1972.

3. Bogorodskiy, V. V., et al., "Slow Ocean Waves," I S"YEZD SOVETSKIKH OKEANOLOGOV, TEZISY DOKLADOV (First Congress of Soviet Oceanologists, Summaries of Reports), Moscow, June 1977.

4. Yermakov, S. A., Pelinovskiy, Ye. N., "On the Theory of Low-Frequency Surface Waves Induced by Internal Waves in the Ocean," IZV. AN SSSR, FAO (News of the USSR Academy of Sciences, Physics of the Atmosphere and Ocean), 12, No 3, 1976.

5. Thorpe, S. A., "On the Shape of Progressive Internal Waves," PHIL. TRANS. ROY. SOC. LONDON, A263, No 1145, 1968.

6. Monin, A. S., Kamenkovich, V. M., Kort, V. G., IZMENCHIVOST' MIROVOGO OKEANA (Variability of the World Ocean), Gidrometeoizdat, 1974.

5303
CSO: 1870

GEOPHYSICS, ASTRONOMY AND SPACE

UDC 551.466.81

INTERNAL WAVES GENERATED BY LOCAL PERTURBATIONS IN A TWO-LAYER STRATIFIED FLUID

Moscow IZVESTIYA AKADEMII NAUK SSSR, FIZIKA ATMOSFERY I OKEANA in Russian Vol 14, No 11, 1978 pp 1222-1228

[Article by I. V. Sturova, Hydrodynamics Institute, Siberian Division USSR Academy of Sciences, submitted for publication 1 November 1977]

[Text] At the present time the authors of [1-3] have investigated the internal waves arising when a submerged inflow and outflow of equal intensity are surrounded by a uniform flow and when there is collapse of a "spot" of partially or completely mixed fluid, for two special models of density stratification of a fluid: 1) for a constant Brent-Väisälä frequency N and 2) in the case of a thin thermocline in which N differs from zero only in a narrow zone. A limiting case of the latter model is a two-layer fluid with a density jump between homogeneous layers [4].

In this paper we examine the more general case of density stratification of a fluid in which the density distribution in an unperturbed state has the form (the y-axis is directed vertically upward)

$$\rho_0(y) = \rho_* \begin{cases} 1 & (-H \le y \le 0), \\ (1+\varepsilon)[1-\alpha(y+H)] & (-\infty < y < -H), \quad \varepsilon, \alpha = \text{const} > 0. \end{cases} \tag{1}$$

Such a density distribution is characteristic for the upper layer of the ocean in tropical and subtropical regions [5]. The assumption that the lower layer is limitless was introduced as a simplification of the problem. It was demonstrated in [1] that with a sufficient distance of the perturbation from the solid boundary the reflection of waves is negligible.

1. We will investigate the stationary problem of the wave movements caused by a point inflow and a point outflow of equal intensity m situated beneath the free surface at the depth h at the distance 2a from one another in a uniform flow of a heavy fluid. The x- and z-axes are situated at the unperturbed free surface in such a way that the x-axis coincides with the direction of the velocity vector of the fluid far upstream. It is assumed that in a case of sufficiently great submergence and a weak stratification the flow around such a combination of an inflow and outflow is equivalent

to flow around an elongated axially symmetric body (similar to an unbounded homogeneous fluid). The radius R of the "presentation area," body elongation d and velocity V of the main flow unambiguously determine the a and m values [2]. A similar plane problem was solved in [6].

In a linear formulation with use of the Boussinesq approximation the equations of motion of a nonviscous incompressible fluid have the form

$$\frac{\partial u}{\partial x}+\frac{\partial v}{\partial y}+\frac{\partial w}{\partial z}=m[\delta(x+a)-\delta(x-a)]\delta(y+h)\delta(z),$$
$$\rho_i V\frac{\partial u}{\partial x}=-\frac{\partial p}{\partial x},\quad \rho_i V\frac{\partial v}{\partial x}=-\frac{\partial p}{\partial y}-g\rho_i, \tag{2}$$
$$\rho_i V\frac{\partial w}{\partial x}=-\frac{\partial p}{\partial z},\quad V\frac{\partial \rho}{\partial x}+v\frac{d\rho_i}{dy}=0$$

with the boundary conditions

$$v_1 = 0 \qquad \text{when } y = 0$$
$$v_1=v_2,\ V(\partial p_1/\partial x)-g\rho_i v_1=V(\partial p_2/\partial x)-(1+\varepsilon)g\rho_i v_2, \qquad \text{when } y = -H$$
$$u,\ v,\ w,\ p,\ \rho\to 0 \qquad \text{when } x^2+y^2+z^2\to\infty$$

Here u, v, w, p, ρ are perturbations of components of the velocity vector in the direction of the x-, y- and z-axes, pressure and density; g is the acceleration of gravity; δ is the Dirac delta function, the subscript 1 pertains to the upper layer, the subscript 2 pertains to the lower layer. The free surface has been replaced by a solid cover, which makes it possible to filter out the surface waves without a significant distortion of the internal waves.

The function $\eta(x, y, z)$, determining the vertical displacement of a fluid particle, satisfies the linearized condition

$$\partial\eta/\partial x=v/V. \tag{3}$$

We reduce equations (2) to a single equation for the function v; we introduce dimensionless variables, as the scale units for length and velocity taking the R and V values. We use the Fourier transforms for the variables x and z with the real parameters μ and ν respectively. For the function f — the double Fourier transform of v, we obtain ordinary differential equations whose solutions have the form:

for case 1 (singularities in the upper layer)

$$f_1=\sigma\{\operatorname{sign}(y+h)e^{k|y+h|}+e^{-k(y+h)}-2\operatorname{ch}kh[(k+D_2)e^{ky}+(k-D_2)e^{-k(2H+y)}]/D\},$$
$$f_2=-4\sigma k\operatorname{ch}kh\exp[k(y+H)-kH]/D,$$

for case 2 (singularities in lower layer)

$$f_1=-4\sigma M(1+\varepsilon)\operatorname{sh} ky\exp[M(H-h)-kH]/D,$$
$$f_2=\sigma[\operatorname{sign}(y+h)e^{-M|y+h|}+(D_1-k-(k+D_1)e^{-2kH}]\exp[M(2H+y-h)]/D],$$

where

$$\sigma=im\sin\mu a,\quad M=(k^2-\varepsilon)^{1/2},\quad D_{1,2}=M+\varepsilon(M\pm\lambda),$$
$$\mu^2=\mu^2+\nu^2,\quad \lambda=\Lambda k^2/\mu^2,\quad \Lambda=gR/V^2,\quad \varepsilon=Sk^2/\mu^2,\quad S=\alpha R\Lambda, \qquad (4)$$
$$D=k+D_2+(k-D_2)e^{-2kH}.$$

Knowing f, from (3) we determine the function ξ -- a double Fourier transform of the η function and we will perform reverse Fourier transforms as in [2]:

$$\eta(r,\varphi,y)=\frac{1}{2\pi^2}\operatorname{Re}\int_0^{\pi/2}d\theta\int_0^{\infty}k\xi(k,\theta,y)[e^{ikr\sin(\theta+\varphi)}+e^{ikr\sin(\theta-\varphi)}]dk, \qquad (5)$$

where the following replacement is made

$$\mu=k\sin\theta,\quad \nu=k\cos\theta,\quad x=r\cos\varphi,\quad z=r\sin\varphi.$$

The integration contour in the complex k-plane runs along the sections for the fictitious and part of the real axis [2], and in accordance with the radiation condition all the real poles are bypassed from below. The poles of the integrand are the roots of equation (4) $D(k,\theta)=0$, and it is easy to show that it has not more than one positive root k_0; with $\varepsilon, S>0$ only in a case when $D(\sqrt{\varepsilon},\theta)\leqslant 0$, with $S=0$ — for $\lambda>1/\varepsilon H$, with $\varepsilon=0$ there are no roots.

For investigating internal waves at great distances from the source of perturbation, in (5) we leave only the single integrals, representing the residue at the point $k=k_0$, and the double integrals, caused by integration along the section for the real axis k.

For an asymptotic evaluation of these integrals when $r\to\infty$ we will use the stationary phase method. First we will examine the single integrals whose stationary points satisfy the equation $\Psi'(\theta)=0$, where $\Psi(\theta)=k_0(\theta)\sin(\theta\pm\varphi)$ and, accordingly,

$$\operatorname{tg}\varphi=\mp G(\theta),\quad G(\theta)=\frac{\operatorname{tg}\theta\,dk_0/d\theta+k_0}{dk_0/d\theta-k_0\operatorname{tg}\theta},\quad \frac{dk}{d\theta}=-\frac{\partial D}{\partial\theta}\Big/\frac{\partial D}{\partial k}. \qquad (6)$$

It is easy to show that when $0<\theta<\pi/2$ the function $G(\theta)$ is always positive and accordingly, the stationary points have only one of the single integrals. In the case when $\varepsilon, S>0$ or when $S=0$, $\varepsilon H\Lambda\geqslant 1$, for $\varphi<\varphi_m$ there are two stationary points $\theta_{1,2}$ ($\theta_1<\theta_m<\theta_2$) when $\varphi=\varphi_m$ -- one multiple stationary point $\theta=\theta_m$, when $\varphi>\varphi_m$ there are no stationary points ($\varphi_m=\operatorname{arctg}G_m$, G_m is the maximum value of the function $G(\theta)$ when $0<\theta<\bar{\theta}$, $\bar{\theta}$ is a root of the equation $D(\sqrt{\varepsilon},\theta)=0$, $G(0)=G(\bar{\theta})=0$, $G_m=(\theta_m)$). If $\varepsilon H\Lambda<1$ when $S=0$, then for $\varphi<\theta.$ ($\theta.=\arcsin\sqrt{\varepsilon H\Lambda}$) there is one stationary point; when $\varphi\ \theta.$ there are no stationary points.

The stationary points of the double integrals are determined from the system of equations $\partial\chi/\partial\zeta = \partial\chi/\partial\gamma = 0$, where

$$\chi(\zeta, \gamma) = [b\cos\zeta + r\sin\zeta\sin(\gamma \pm \varphi)]/\sin\gamma, \quad b = \text{const} > 0. \tag{7}$$

When $0 < \zeta$, $\gamma < \pi/2$ they exist only for the lower sign and are equal to

$$\zeta_0 = \arcsin\frac{bx}{[(x^2+b^2)(x^2+z^2+b^2)]^{1/2}}, \quad \gamma_0 = \operatorname{arctg}\frac{b^2+z^2}{xz}.$$

The final expressions for the function $\eta(x, y, z)$ have the form:

for case 1

$$\eta_1 = \sum_{i=1}^{3} A(k_i, \theta_i)B(k_i)C(k_i)(k_i - D_2(k_i)),$$

$$\eta_2 = 2\sum_{i=1}^{3} k_i A(k_i, \theta_i)B(k_i)e^{M_i(y+H)} - \frac{\sqrt{S}\,\sigma_1\sin 2\zeta_1}{\sin\gamma_1(c_1^2+d_1^2)}(c_1\cos\chi_1 - d_1\sin\chi_1) \tag{8}$$

$$\times\{\exp[\sqrt{S}(h-H)\sin\zeta_1/\sin\gamma_1] + \exp[-\sqrt{S}(h+H)\sin\zeta_1/\sin\gamma_1]\},$$

for case 2

$$\eta_1 = -2(1+\varepsilon)\sum_{i=1}^{3} M_i A(k_i, \theta_i)C(k_i)e^{M_i(H-h)} + \frac{2\sqrt{S}\sigma_2(1+\varepsilon)\cos^2\zeta_2}{\sin\gamma_2(c_2^2+d_2^2)}(c_2\sin\chi_2 + d_2\cos\chi_2)\times$$

$$\times\{\exp[-\sqrt{S}(y+H)\sin\zeta_2/\sin\gamma_2] - \exp[\sqrt{S}(y-H)\sin\zeta_2/\sin\gamma_2]\},$$

$$\eta_2 = -2(1+\varepsilon)\sum_{i=1}^{3} M_i A(k_i, \theta_i)(1 - e^{-2h_i H})e^{M_i(2H-h+y)} +$$

$$+ \frac{\sigma_2\cos\zeta_2}{c_2^2+d_2^2}[2c_2d_2\sin\chi_2 - (c_2^2-d_2^2)\cos\chi_2] + \operatorname{sign}(h+y)\sigma_1\cos\zeta_1\cos\chi_1.$$

Here k_i is a root of the equation $D(k, \theta_i) = 0$,

$$A(k, \theta) = m\sqrt{\frac{2}{\pi r}}\frac{\sin(ak\sin\theta)}{\sin\theta\sqrt{\gamma|P|}}\sin[rk\sin(\theta-\varphi) + \operatorname{sign}P\pi/4],$$

$$B(k) = e^{h(h-H)} + e^{-h(h+H)}, \quad C(k) = e^{-h(H+y)} - e^{h(y-H)},$$

$$M_i = \sqrt{k_i^2 - S/\sin^2\theta_i}, \quad \gamma = dD/dk|_{k=k_i}, \quad P = d^2\Psi/d\theta^2|_{\theta=\theta_i}.$$

ζ_n, γ_n ($n = 1, \ldots, 4$) are the critical points of the function χ in (7) when $b = b_n$,

$$b_1 = |y|, \quad b_2 = h - H, \quad b_3 = h - y - 2H, \quad b_4 = |h+y|, \tag{9}$$

$$\sigma_n = \frac{m \sin(\alpha\sqrt{S}\sin\zeta_n)}{\pi(z^2+b_n^2)^{1/4}}, \quad \chi_n = b_n\left[\frac{S(z^2+z^2+b_n^2)}{z^2+b_n^2}\right]^{1/4},$$

$$c_n = [\sqrt{S}\sin\zeta_n - \varepsilon\Lambda/\sin\gamma_n + (\sqrt{S}\sin\zeta_n + \varepsilon\Lambda/\sin\gamma_n)\exp(-2\sqrt{S}H\sin\zeta_n/\sin\gamma_n)]/\sin\gamma_n, \tag{9}$$

$$d_n = (1+\varepsilon)\sqrt{S}\cos\zeta_n[1-\exp(-2\sqrt{S}H\sin\zeta_n/\sin\gamma_n)]/\sin\gamma_n.$$

Similar expressions are also obtained for the other sought-for functions, in particular, the horizontal components of velocity at the free surface when $H > 0$ are equal to:

for case 1

$$u_1(x,0,z) = \sum_{i=1}^{2} K(k_i,\theta_i)\sin\theta_i, \quad w_1(x,0,z) = -\sum_{i=1}^{2} K(k_i,\theta_i)\cos\theta_i,$$

for case 2

$$u_1(x,0,z) = \sum_{i=1}^{2} L(k_i,\theta_i)\sin\theta_i + T_2\sin\gamma_2,$$

$$w_1(x,0,z) = -\sum_{i=1}^{2} L(k_i,\theta_i)\cos\theta_i - T_2\cos\gamma_2,$$

where

$$K(k,\theta) = 2k\sin\theta(k-D_2)A(k,\theta)B(k)e^{-kH},$$

$$L(k,\theta) = -4(1+\varepsilon)kM\sin\theta A(k,\theta)\exp[M(H-h)-kH],$$

$$T_2 = \frac{4S\sin\zeta_2\cos^2\zeta_2}{\sin\gamma_2(c_2^2+d_2^2)}(1+\varepsilon)\sigma_2(c_2\sin\chi_2+d_2\cos\chi_2)\exp(-\sqrt{S}H\sin\zeta_2/\sin\gamma_2).$$

For the special cases $H = 0$ or $S = 0$ expressions (8) coincide with the known solutions [1, 4]. It should be noted that these solutions are not uniformly correct for φ in the neighborhood of the boundaries $|\varphi| = \bar{\theta}$, $|\varphi| = \theta_m$, $|\varphi| = \theta$. of the wave zones, and also the ray $\varphi = 0$. With such parameters it is necessary that the results obtained above be refined.

In Figures 1a and 1b we show isolines of the function $50\eta/R$ for $x/R = 150$, $H/R = 5$, $h/R = 10$, $d = 10$, $S = 0.01$, $\Lambda = 100$, $\varepsilon = 0$; 0.001. The roots of the equations $D(k, \theta) = 0$ and (6) were determined numerically.

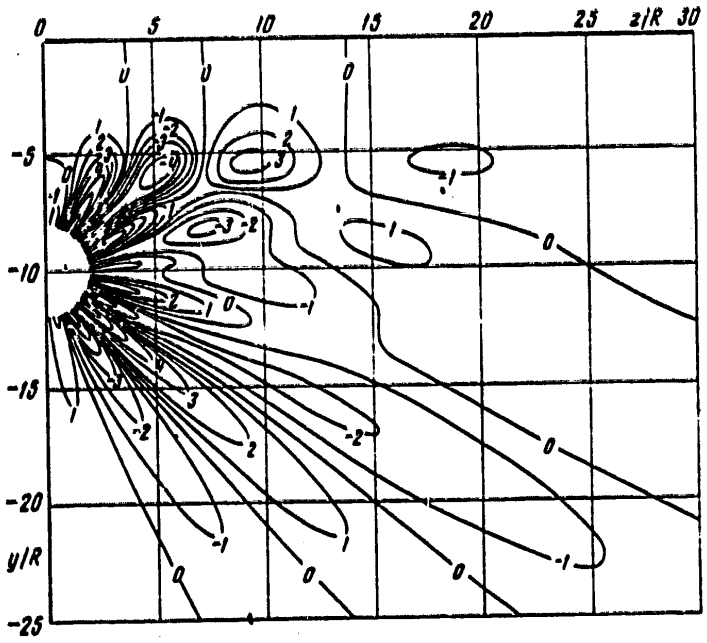

Fig. 1a. Isolines of function $50\eta/R$ with interval 1 for x/R = 150, H/R = 5, h/R = 10, d = 10, S = 0.01, Λ = 100, ε = 0

With a positioning of the singularities in the upper layer and absence of a density jump the internal waves are negligible, but with an increase in ε considerable wave disturbances can arise in the lower layer of the fluid both in the neighborhood of the discontinuity and far from it.

2. Now we will examine the plane nonstationary problem of a current arising during collapse of an initially circular spot of the radius R in a completely or partially mixed fluid surrounded by a stratified fluid. As indicated in [7], the properties of such a current are intimately linked to the behavior of turbulent regions arising in wakes or during the collapse of internal waves, and the fine structure of the vertical distribution of density and velocity gradients in the ocean and atmosphere.

At the initial moment in time t = 0 the density perturbation has the form

$$\rho(y,z,0)=\begin{cases}\beta\alpha(y+h)\rho_0(-H) & (\gamma\sqrt{(y+h)^2+z^2}<R),\\ 0 & (\gamma\sqrt{(y+h)^2+z^2}>R),\end{cases}\quad 0<\beta\leqslant 1$$

in the case of a completely mixed spot β = 1. Outside the spot the density distribution is determined (1) and it is assumed that h > H + R. The method for solving this problem is similar to that set forth in Section 1 (the time

t plays the role of the longitudinal coordinate x; for the scale units of length and time we used the values R and $1/\sqrt{\alpha g}$.

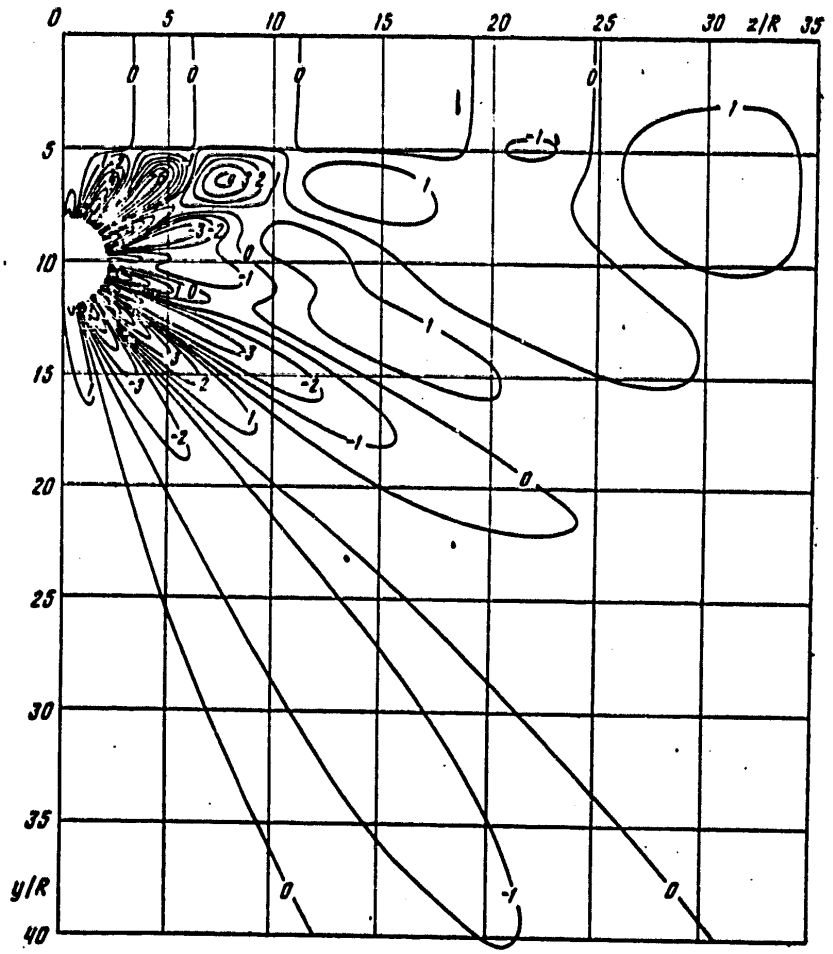

Fig. 1b. Same as in Fig. 1a for $\varepsilon = 0.001$

The final expressions for the function $\eta(y, z, t)$ outside the spot have the form

$$\eta_1 = \sum_{i=1}^{n} A(k_i, \theta_i)\exp[M_i(H-h)]\{\exp[-k_i\cos\theta_i(H+y)] - \exp[k_i\cos\theta_i(y-H)]\} -$$
$$- \frac{2(1+\varepsilon)}{c_2^2+d_2^2}\sigma_2\cos\zeta_2\operatorname{ctg}\gamma_2(c_2\cos\chi_2 - d_2\sin\chi_2)\{\exp[-\sin\zeta_2\operatorname{ctg}\gamma_2(H+y)] -$$
$$- \exp[\sin\zeta_2\operatorname{ctg}\gamma_2(y-H)]\},$$

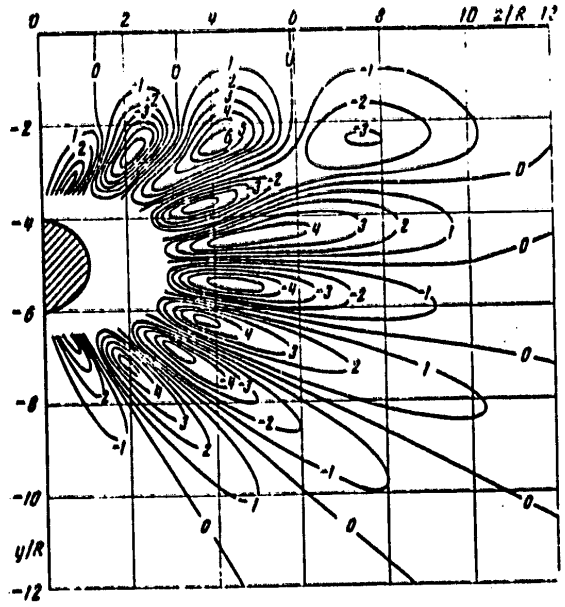

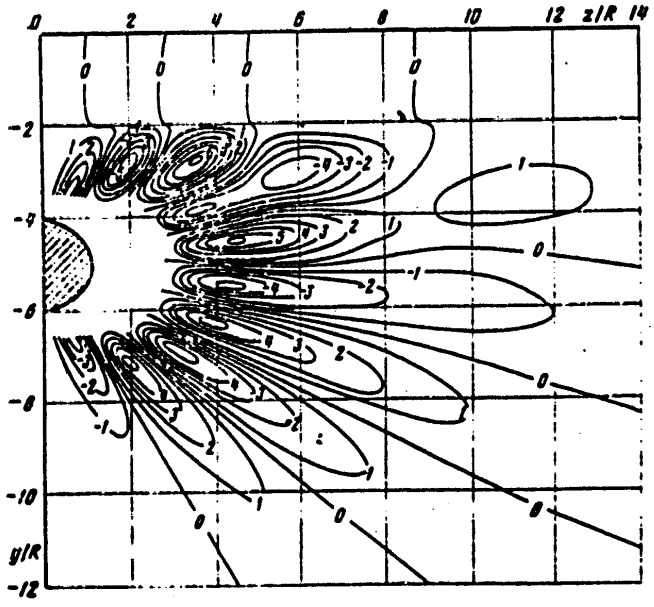

Fig. 2. Caption on following page

Caption for Figure 2: Isolines of function $50\eta/R$ with interval 1 for $t\sqrt{\alpha g} = 15$, $\Lambda = 5000$, $H/R = 2$, $h/R = 5$, $\beta = 1$: a -- $\varepsilon = 0$, b -- $\varepsilon = 0.001$. The shaded semicircle corresponds to the initial position of the spot. The current is not shown in the neighborhood of the spot due to the merging of the lines.

$$\eta_2 = \sum_{i=1}^{2} A(k_i, \theta_i)(1-e^{-2k_iH\cos\theta_i})\exp[M_i(2H+y-h)] -$$

$$- \frac{\sigma_2}{c_2^2+d_2^2}(2c_2d_2\cos\chi_2 + (c_2^2-d_2^2)\sin\chi_2] + \operatorname{sign}(y+h)\sigma_4\sin\chi_4.$$

Here k_i is a root of the equation

$$D(k, \theta_i) = k\cos\theta_i + D_2 + (k\cos\theta_i - D_2)e^{-2kH\cos\theta_i} = 0,$$

$$A(k,\theta) = 2\beta\sqrt{\frac{2\pi}{r}}(1+\varepsilon)\frac{MJ_2(\operatorname{ctg}\theta)}{\sin\theta T\gamma|P|}\cos(rk\sin(\theta-\varphi) + \operatorname{sign}P\pi/4),$$

$$T = dD/dk|_{k=k_i}, \qquad P = d^2\Psi/d\theta^2|_{\theta=\theta_i},$$

$$M_i = \cos\theta_i\sqrt{k_i^2 - 1/\sin^2\theta_i}, \qquad D_2 = M + \varepsilon(M - \Lambda\operatorname{ctg}^2\theta),$$

$\Lambda = 1/\alpha R$, ζ_n, γ_n are critical points of the function

$$\chi(\zeta, \gamma) = [b_n\cos\gamma\cos\zeta + r\sin\zeta\sin(\gamma-\varphi)]/\sin\gamma,$$

equal to

$$\zeta_n = \operatorname{arctg}(b_n/z), \quad \gamma_n = \operatorname{arctg}[(b_n^2+z^2)/zt]; \quad b_2, b_3, b_4$$

b_2, b_3, b_4 were determined in (9),

$$\chi_n = t\sin\zeta_n, \qquad \sigma_n = \beta\operatorname{ctg}\gamma_n J_2(\operatorname{ctg}\gamma_n)/t,$$

$$c_n = \cos\gamma_n\left[k_n - \frac{\varepsilon\Lambda\operatorname{ctg}\gamma_n}{\sin\gamma_n} + \left(k_n + \frac{\varepsilon\Lambda\operatorname{ctg}\gamma_n}{\sin\gamma_n}\right)e^{-2k_nH\cos\gamma_n}\right],$$

$$d_n = (1+\varepsilon)\cos\zeta_n\operatorname{ctg}\gamma_n(1-e^{-2k_nH\cos\gamma_n});$$

J_2 is a second-order Bessel function of the first kind.

The horizontal velocity w at the free surface, when $H > 0$, is equal to

$$w(0,z,t) = -4\beta\sqrt{\frac{2\pi}{r}}(1+\varepsilon)\sum_{i=1}^{2}\frac{k_iM_i}{T\gamma|P|}J_2(\operatorname{ctg}\theta_i)\exp[-(M_ih + k_iH\cos\theta_i)]\times$$

$$\times\cos(rk_i\sin(\theta_i-\varphi) + \operatorname{sign}P\pi/4) +$$

$$+\frac{2(1+\varepsilon)\sigma_2}{c_2^2+d_2^2}\sin 2\zeta_2\operatorname{ctg}\gamma_2\exp(-H\sin\zeta_2\operatorname{ctg}\gamma_2)(c_2\cos\chi_2 - d_2\sin\chi_2).$$

Figure 2 shows isolines of the function $50\eta/R$ for $t\sqrt{\alpha g} = 15$, $\Lambda = 5000$, $H/R = 2$, $h/R = 5$, $\vartheta = 1$, $\varepsilon = 0$; 0.001. It is interesting to note that in the presence of a density jump the internal waves generated by a collapse of the mixing zone virtually will not distort the form of the discontinuity along its entire length, whereas for internal waves from a body (compare Fig. 1,b) this is observed only near the axis of the wake.

BIBLIOGRAPHY

1. Miles, J. W., "Internal Waves Generated by Horizontally Moving Source," GEOPHYS. FLUID DYN., 2, No 1, 1971.

2. Sturova, I. V., "Wave Movements Arising in a Stratified Fluid During Flow Around a Submerged Body," PMTF (Applied Mathematics and Theoretical Physics), No 6, 1974.

3. Hartman, R. I., Lewis, H. W., "Wake Collapse in a Stratified Fluid: Linear Treatment," J. FLUID MECH., 51, Part 3, 1972.

4. Sturova, I. V., "Wave Movements Arising from a Stepped Stratification During Flow Around a Submerged Body," CHISLENNYYE METODY MEKHANIKI SPLOSHNOY SREDY (Numerical Methods in the Mechanics of a Continuous Medium), Vol 6, No 3, Novosibirsk, Izd-vo VTs SO AN SSSR, 1975.

5. Phillips, O., DINAMIKA VERKHNEGO SLOYA OKEANA (Dynamics of the Upper Layer of the Ocean), "Mir," 1969.

6. Sturova, I. V., "Plane Problem of Wave Movements Arising in a Stratified Fluid During Flow Around a Submerged Dipole," DINAMIKA SPLOSHNOY SREDY (Dynamics of a Continuous Medium), No 14, Novosibirsk, Izd. In-ta Gidrodinamiki SO AN SSSR, 1973.

7. Bell, T. H., Dugan, J. P., "Model for Mixed Region Collapse in a Stratified Fluid," J. ENG. MATH., 8, No 3, 1974.

5303
CSO: 1870

SCIENTISTS AND SCIENTIFIC ORGANIZATIONS

VSEVOLOD VLADIMIROVICH FEDYNSKIY (OBITUARY)

Moscow ASTRONOMICHESKIY VESTNIK in Russian Vol 12, No 4, 1978 pp 247-249

[Text] Associate Member of the Academy of Sciences of the USSR Vsevolod Vladimirovich Fedynskiy, editor-in-chief of "Astronomicheskiy Vestnik," died suddenly on 17 June 1978. This marks the passing of a great scientist, an eminent specialist in the area of physics of the earth, exploratory geophysics, meteor astronomy, an excellent organizer of science.

V. V. Fedynskiy was born on 1 May 1908 in Mirgorod in a physician's family. From his early years he was interested in astronomy, observed the great opposition of Mars in 1924 with a small telescope, and the next year entered the mechanics and mathematics department of Moscow University from which he graduated in 1930 with a major in astronomy and gravimetry. As early as 1927 V. V. Fedynskiy had organized a meteor division of the Collective of Observers of the Moscow Society of Amateurs of Astronomy (later to be the Moscow Department of the All-Union Astronomical-Geodetic Society). This division started a systematic study of meteor showers, first from visual observations, and then on the initiative of V. V. Fedynskiy the photographic and spectral study of meteors was begun. In 1932 V. V. Fedynskiy and K. P. Stanyukovich obtained and analyzed a basis photograph of a bright meteor, and used it to determine the distribution of temperature of the atmosphere with respect to altitude at the 80-100 km level. In 1934, a group of observers under the guidance of V. V. Fedynskiy obtained a bright meteor spectrum of 47 lines. In 1937, the first meteor patrol in the USSR was set up and used as the base for development of a stationary meteor patrol set up at the observatory in Dushanbe. V. V. Fedynskiy made a great contribution to the development of meteoric methods of studying the upper layers of the atmosphere. One of these methods is the observation of the drift of meteor trails. These observations were first made visually, and then by photography, and most recently, with the active participation of V. V. Fedynskiy, radar methods of studying the drift of meteor trails have been developed.

The results of these studies was a monograph written by V. V. Fedynskiy jointly with P. B. Babadzhanov, B. L. Kashcheyev and V. A. Nechitaylenko, "Radiometeor Studies of the Circulation of the Upper Atmosphere" (Dushanbe, 1974). This book summarized the results of the Soviet Equatorial Meteor Expedition of 1968-1970.

V. V. Fedynskiy had a reputation as the organizer of meteor research in the USSR. From the year 1958 he was the head of the commission on meteors of the Astronomy Council of the Academy of Sciences of the USSR, and for six years (1958-1964) was the president of Commission No 22 of the International Astronomical Union (on meteor astronomy). Until the end of his life he was the head of the meteor section of the Interdepartmental Geophysical Committee affiliated with the Presidium of the Academy of Sciences of the USSR.

After completing the university, V. V. Fedynskiy started work as the chief of gravimetric detachments in Azerbaydzhan, Dagestan, Turkmenia and in Povolzh'ye (he had been making gravimetric measurements while he was still a student). In 1936 he had been designated technical director of the gravimetric method of mineral prospecting of the State Union Geophysics Trust. During the war, field detachments of this trust prospected for oil and other natural riches, using various geophysical methods: gravimetric, electric logging and others. New deposits were discovered. V. V. Fedynskiy strove to introduce new methods and instruments, and in particular to replace the inconvenient pendulum instruments in gravimetry. For developing and introducing Soviet gravimeters, V. V. Fedynskiy was awarded the State Prize in 1951. Simultaneously with the development of gravimeter designs, V. V. Fedynskiy was the director of the Scientific Research Institute of Applied Geophysics (1943-1952). In 1952 he was named chief of Glavneftegeofizika of the Ministry of the Petroleum Industry of the USSR. From 1957 he was the chief of the department, and then the Administration of Geophysical Work of the Ministry of Geology of the USSR, where he worked until 1977.

V. V. Fedynskiy organized the service of marine geophysical work of the Pacific Ocean and Antarctica. He was much involved in the theory and

practice of marine gravimetry, developed methods of complex geophysical studies, organized searches for new deposits of petroleum and natural gas, participated in the organization of ultradeep drilling. He wrote the fundamental work "Exploratory Geophysics" that was published in 1965 and was republished many times. Although this book is required as a text for students majoring in geophysics and geology, at the same time it is also a monograph on this topic that is necessary for specialists as well.

In his scientific work, V. V. Fedynskiy was able to successfully combine his own knowledge and interests in different areas of science. As early as 1947 he published an important theoretical work "On the Destructive Action of Meteor Strikes" (jointly with K. P. Stanyukovich). In this work, V. V. Fedynskiy and K. P. Stanyukovich predicted the existence of craters on the moon long in advance of Western scientists. In recent years V. V. Fedynskiy had turned to the problem of crater formation on planets. The discovery of gigantic crater structures on the earth and proof of their impact origin on many planets of the solar system stimulated him to consider the problem of evolution of crater formations over prolonged periods (millions of years or more) under the action of various geophysical processes (isostatic leveling and so forth). Together with his students (M. S. Krass, A. I. Dabizha, Yu. I. Fadeyev) he made an analysis of this problem and derived interesting results. At the present time, Nauka Press is preparing to publish a collective monograph "Meteoric Structures on the Surfaces of Planets" edited by V. V. Fedynskiy.

From 1956, V. V. Fedynskiy was a professor in the geology department of Moscow State University, and from 1957 was head of the department of geophysical methods of studying the earth's crust, while in his last years he headed the geophysics division of the department.

He gave courses in gravimetric prospecting and the theory of the gravitational potential. Of his geophysicist students, 20 have become candidates of sciences, and three have become doctors of sciences. Vsevolod Vladimirovich trained many students in the field of meteor astronomy as well.

Since his youth he was an active member of the All-Union Astronomical-Geodetic Society, and in various years was the head of the meteor division, chairman of the Collective of Observers of the Moscow Division of the All-Union Astronomical-Geodetic Society, and from 1967 to his death was editor-in-chief of "Astronomicheskiy Vestnik." In 1970 he was elected an honorary member of the Society and first vice-president of the All-Union Astronomical-Geodetic Society. He was a member of the CPSU since 1942.

The memory of Fedynskiy -- scientist, organizer, pedagog, editor, educator of young people, a sensitive and sympathetic man -- will live in the hearts of all those who had the pleasure of working at his side or profiting from his council and assistance.

6610
CSO: 1870

PUBLICATIONS

THE 'EPOS' ELECTRONIC CALCULATOR

Moscow ELEKTRONIKA EPOS (POSOBIYA DLYA RABOTNIKOV MASHINOSCHETNYKH BYURO) (The Epos Electronic Calculator--Textbooks for Employees of Machine Accounting Bureaus) in Russian 1978 signed to press 28 Feb 78 pp 5, 79, 92-94

[Annotation, table of contents, photo caption on p 5 and explanatory text on p 79 for photo on p 80 from book by A. M. Baraboshkin, Statistika, 24,000 copies, 93 pages]

[Text] The book considers the technical characteristics and block diagrams of the Epos electronic calculating machine, elements of the functional diagram, the structure and function of the functional units of the machine, the operational algorithms, and the construction and maintenance of the machine.

The book is intended for employees of computer installations--machine accounting bureaus, computer centers, and machine accounting stations.

It will be useful to students studying electronic computer technology in VUZ's and tekhnikums.

Contents

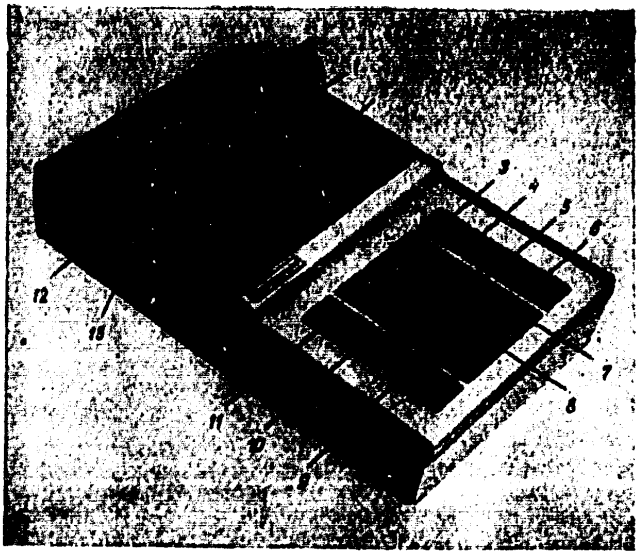

Figure 1.1. General View of the Elektronika Epos Electronic Calculating Machine:

1. Numeric information display
2. Button to turn on the machine
3. Division key
4. Multiplication key
5. Subtraction key
6. Addition key
8. Digital keyboard
9. Result key
10. Reset key
11. Correction key (key to clear information from the display register
12. Negative result indicator
13. Overflow indicator

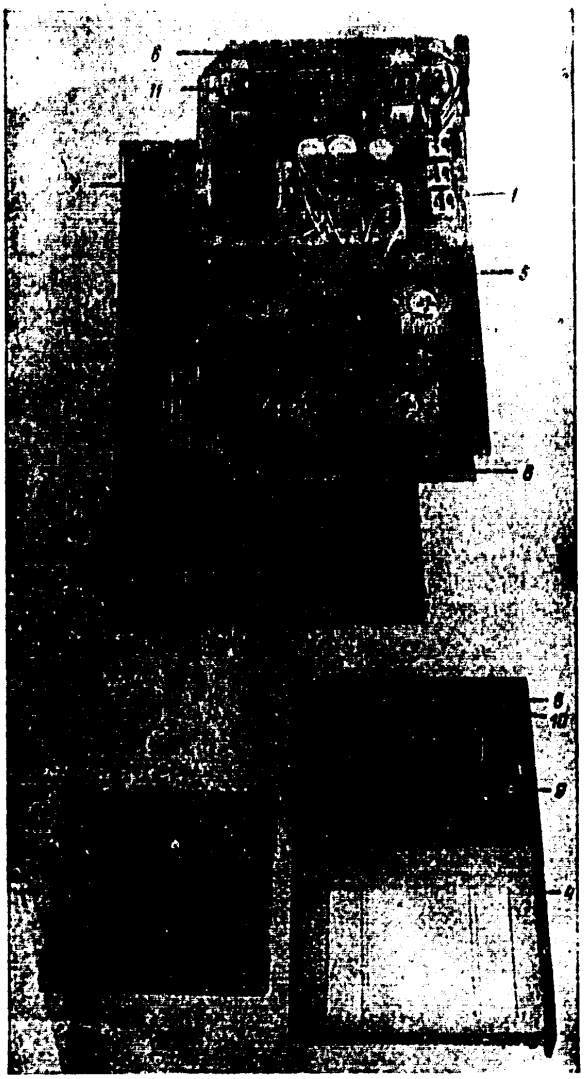

The construction of the Elektronika Epos machine includes (figure 5.1.) board 1 -- the output display device, board 2 -- the input key device; case 3 and cover 4. On board 1 are mounted four large integrated circuit circuits (series K145 microcircuits), a BPZ power power unit in the form of a separate device, an IV-18 display, K2LN641 keys for controlling the anodes and matrices of the display, and three series K172 microcircuits to

eliminate false lighting in the display. Board 1 also provides a place for mounting the power unit on discrete elements. On board 2 three keyboard units are mounted forming a pegboard:
VM16-1 -- digit keys and decimal point
VM16-4 -- "+", "-", "x", and "÷" keys
VM16-6 -- "S", "SK", and "=" keys
and the phase generator in the form of a K1GF651 microcircuit.

Board 2 also provides room for mounting a phase generator made up of discrete elements. Board 1 and board 2, forming a combined unit, are connected to each other with two MRN-22 (5) type connectors attached to the edges of the boards. The combined unit is attached to the case by screws (opening 6) and is closed with a cover which is attached to the case with screws (opening 7). Special openings (8) are provided in the case and cover to permit the operator to establish the necessary angle of inclination of the machine to facilitate computation of data. The open position of the stand at the same time improves heat exhaust from the machine on the sides of the case. On the face side of the cover is located the on-off button (9), the pressing of which opens the cover (10) and permits access to the digit display (11).

8542
CSO: 1870

PUBLICATIONS

UDC 621.791.4:621.771

ROLL WELDING OF BIMETALS

Moscow SVARKA PROKATKOY BIMETALLOV in Russian 1977 pp 2, 4-6, 157-158

[Annotation, Introduction and Table of Contents of book by Sergey Aleksandrovich Golovanenko, Izdatel'stvo Metallurgiya, signed to press 31 August 1977, 4,900 copies, 158 pages]

[Text] ANNOTATION

The author discusses the physicochemical processes taking place in the zone where the materials are joined during the production of bimetals by hot and cold roll welding.

He describes the production processes involved in obtaining bimetals of various types for various purposes, as well as the principles governing the designing of corrosion-resistant bimetals and the selection of materials for the intermediate layers, which principles are based on a thermodynamic analysis of the carbon redistribution processes in the zone where steels of different classes are joined together.

This book is intended for scientific and engineering and technical personnel specializing in the production, use, development, and investigation of bimetals and compound materials for different purposes. It can also be useful for students and graduate students in technical VUZ's. Illustrations 69; tables 18; bibliography of 148 titles.

INTRODUCTION

The development of modern technology is inextricably related to the increasing use of metallic materials, the requirements for which -- from the viewpoint of insuring reliability and durability, economy and technological qualities -- are steadily increasing because of the intensification of thermal effects, increasing mechanical loads and working medium aggressiveness, and so on.

In particular, the functional characteristics of metallic materials can be improved by the development and industrial adoption of bimetallic and composite (combined) materials.

Bimetallic and multilayer rolled stock is one of the most progressive and economical forms of metallurgical production, and it is being used more and more widely in many branches of the national economy. The need for increasing the volume of its production and enlarging the assortment of available products follows from the assignment given metallurgists by the 25th CPSU Congress: to increase the output of effective types of metal products.

Over the last decade, the production and consumption of bimetals in our country has increased by 50 percent. There has been a particularly sharp increase in the consumption of two-layer corrosion-resistant steel -- it has more than doubled.

At the present time the consumption of bimetal is relatively small in comparison with the total steel output (about 0.1 percent), but it plays a very large role. In connection with this, bimetal can be used both as a replacement for uniform metals and as a material with a new complex of functional or technological characteristics.

An example of the creation of a new complex of properties by combining specially selected steels is self-sharpening sheet and shaped bimetallic rolled stock. It is used in agricultural cultivating and digging machines. Self-sharpening during operation of a plowshare, plow, cultivator blade, shallow plow disk, and so on, is insured as the result of the sharply different rate of wear of the soft and hard layers when the soil acts abrasively on the cutting element. The relationship of the bimetal components' wear rates must be determined exactly, and it depends on the wear resistance of the steels and their thickness. Self-sharpening of the elements of soil-working machines makes it possible to reduce expenses for honing and replacing parts, as well as the force required; that is, the amount of fuel consumed during plowing, cultivating and other soil work.

Another example of the new complex of properties that are realized in layered metallic materials are the so-called thermoelastic bimetals (or thermobimetals). These bimetals consist of two layers of steels or alloys with substantially different coefficients of thermal expansion. When a piece of the bimetal is heated, this factor leads to considerable bending of the bimetallic element, with the magnitude of the flexure depending on the heating temperature. These bimetallic elements are widely used in instruments for measuring and regulating

temperature and protecting electrical circuits from overloading, as well as other similar situations.

In the electrical engineering industry there is a constant expansion of the use of the effect of superconductivity, which is a property possessed by a number of alloys of refractory and rare metals and their chemical compounds (the intermetallides). Copper is not a superconductor but, since it has a high thermal conductivity rating, when it is combined with a superconductive material it is an ideal structural material for the creation of strong magnetic fields.

All these examples show how diversified the functional properties of bimetals can be.

The development of bimetals with a completely new set of functional properties is a promising area of the modern science of materials, since it raises the possibility of reaching completely new and original structural decisions for machines, equipment and instruments.

In this book we correlate the results of work done by the author and his coworkers at the Central Scientific Research Institute of Ferrous Metallurgy imeni I.P. Bardin and in the laboratories at a number of Soviet metallurgical plants under production conditions. Use is also made of the most interesting results published in periodicals.

The author wishes to express his gratitude to Candidates of Technical Sciences A.A. Bykov and I.Yu. Konnova, as well as to engineer A.M. Logvinova, for their great assistance in the preparation of the manuscript and their active participation in the discussion of its separate parts.

The author is indebted to the collective of the Bimetals Laboratory of the Central Scientific Research Institute of Ferrous Metallurgy imeni I.P. Bardin for its assitance in conducting experiments.

TABLE OF CONTENTS

11746
CSO: 1870

PUBLICATIONS

UDC 621.039.5.053+621.039.553.36

CORROSION OF STRUCTURAL MATERIALS IN MOLTEN ALKALINE METALS

Moscow KORROZIYA KONSTRUKTSIONNYKH MATERIALOV V ZHIDKIKH SHCHELOCHNYKH METALLOV in Russian 1977 pp 2-4, 262-263

[Annotation, Foreword and Table of Contents of book by Boris Aleksandrovich Nevzorov, Vitaliy Vasil'yevich Zotov, Vladimir Alekseyevich Ivanov, Oleg Viktorovich Starkov, Nikolay Dmitriyevich Krayev, Yevgeniy Vasil'yevich Umnyashkin, and Vladislav Aleksandrovich Solov'yev, Izdatel'stvo Atomizdat, signed to press 17 May 1977, 2,320 copies, 264 pages]

[Text] ANNOTATION

The authors present primarily original experimental and theoretical material on the corrosive interaction of structural steels and alloys with molten alkaline heat-transfer agents (sodium, sodium-potassium alloy and lithium). The kinetics of their interaction are described, and there is a discussion of different models of the mass transfer process in a nonisothermic circuit system. The authors evaluate the basic factors affecting the mass transfer process, such as the heat-transfer agent's rate of movement, temperature, flow rate, the geometry of the stand, and others. They explain the basic principles of the alloying of steels for the purpose of reducing their rate of dissolution in alkaline metals.

This book is intended for the use of scientific workers and specialists on corrosion and the science of materials, as well as for technologists, developers and planners working in the fields of atomic and power engineering. Figures 88; tables 71; bibliography of 254 titles.

FOREWORD

B.A. Nevzorov's book "Corrosion of Structural Materials in Sodium," which was basically devoted to the experimental study of the mechanisms of corrosion, was published in 1968. Using

sodium as an example, he developed a physicochemical approach to the explanation of the effect on corrosion of such nonmetallic impurities as oxygen and hydrogen. In the book he presented the results of corrosion tests and investigations of the basic classes of structural materials in a sodium heat-transfer agent for the purpose of studying the mechanism of corrosion, as well as to establish the relationship between the corrosion resistance of materials and their chemical composition.

The present book, which was written by a large collective of authors, retains some of the continuity of the 1968 book, but at the same time is more multifaceted with respect to the techniques used in the investigations and includes new theoretical developments and correlations.

The collective of authors that worked on this book considers it its duty to emphasize that in the development of the science of materials for high-temperature, molten metal heat-transfer agents, Doctor of Chemical Sciences Professor Vasiliy Savvich Lyashenko made a significant pioneering contribution. Besides this, it is necessary to mention that the research discussed in this book was stimulated by the constant interest in the study of the behavior of structural materials in molten metal heat-transfer agents that was expressed by A.I. Leypunskiy, academician of the Ukrainian SSR Academy of Sciences.

During the period when this book was being prepared for publication, Doctor of Technical Sciences Professor B.A. Nevzorov, a leading specialist in the corrosion of structural materials in molten metal heat-transfer agents, died. Research in the corrosion of structural materials in sodium was begun in our country by a collective of workers led by V.S. Lyashenko and B.A. Nevzorov. Simultaneously with the development of testing methods and the mastery of the technology and techniques for working with a heat-transfer agent so unusual in power engineering as molten sodium, B.A. Nevzorov's initiative led to the beginning of research in the physicochemical phenomena and processes taking place in a structural material-sodium system. The collective's achievements in studying the corrosion mechanisms of structural materials in molten metals and in recognizing the general regularities of corrosion processes were largely determined by the fruitful creative leadership of B.A. Nevzorov.

The authors dedicate this book to the memory of these scientists.

TABLE OF CONTENTS

11746
CSO: 1870

PUBLICATIONS

TABLE OF CONTENTS FROM JOURNAL 'EXPLORATORY GEOPHYSICS'

Moscow RAZVEDOCHNAYA GEOFIZIKA in Russian No 79, 1977 signed to press 26 Aug 77 pp 164-165

[Table of contents from publication edited by V. Yu. Zaychenko, Izdatel'stvo Nedra, 2,800 copies, 169 pages]

[Text] Contents Page

9082
CSO: 1870

END